Groundwater Cleanup Using Photocatalysis

By

Michelle Jane Stewart (Pembroke)

Fourth-year Undergraduate Project

In Group D, 2011/2012

I hereby declare that, except where specifically indicated, the work submitted herein is my own original work.

Signed:

Date:

Groundwater Cleanup Using Photocatalysis

Michelle Jane Stewart (Pembroke)

Technical Abstract

This report investigates the feasibility of using ActivGlass self-cleaning window glass in photocatalytic groundwater remediation. Groundwater is an important source of our daily freshwater need. However, it is also one of the easiest to be polluted and often undetected as it is out of sight. As a result, current groundwater clean-up technologies are often inefficient, expensive, complex and hard to control, yet still inconclusive. Thus, there is great need for a clean and cost-effective in-situ groundwater clean-up technology that works. Photocatalysis is a promising new alternative technology to fill this gap but current systems are hampered by the difficulty in immobilising the P25 catalyst widely used in slurry reactors as well as the cost factors pertaining the light source and catalyst manufacture. ActivGlass manufactured by the Pilkington Glass Company is a new commercially available self-cleaning window glass using a film coated photocatalyst. This projects aims to test the feasibility of using this glass as the catalyst in propsed photocatalytic reactor designs by subjecting it to various experiments under changing initial conditions. Following that, it hopes to establish the limiting factors of the reaction and use that information to propose a design configuration to maximise pollutant removal, which needs to be tested further.

The report is split into 5 sections and brief summaries of each as below:

1) **Introduction**

The motivation for the project was explored here by assessing groundwater pollution and pollutants as well as the various current groundwater treatment technologies plus currently proposed photocatalytic reactor designs too. This section covers why and where current systems for groundwater clean-up systems fall short, introducing photocatalysis as a promising new alternative that is environmentally friendly and cost effective.

2) **Theory and Literature Review**

Section 2 analyses the photocatalytic process further through an extensive literature review on the photocatalytic mechanism, the Titanium Dioxide (TiO_2) catalyst, ActivGlass and the use of Methylene Blue (MB) dye as a proxy for organic contaminants in the groundwater. Theoretical expectations of the degradation efficiency of pollutants/dye due to several different factors were also summarised for comparison with the results obtained further on.

3) **Experimental Design, Technique and Apparatus**

Moving on, the experimental design, technique and apparatus were detailed in Section 3. The experimental method was split into 3 main types of tests: calibration, small tank reactor tests and other tests. A section on the experimental accuracy of the tests was also included.

4) Results and Discussion

All the measurements tabulated from the various experiments were presented here in graphical form, and its results analysed and discussed in detail. These results include: an absorption-concentration calibration, measurements of the UV/Visible spectra for both the ActivGlass and dye at initial concentration, effects of evaporation, solution volume, light intensity and aeration. On top of that, a layered photocatalytic reactor design was also proposed and a series of further tests were done to analyse this configuration.

5) Conclusions and Suggestions for Future Work

Based on the results and discussions in Section 4, it was concluded that ActivGlass was a good replacement for the P25 catalysts used previously. The layered configuration should also work well in practice as it satisfied the limiting factors identified.

The main experimental technique used in this project was in the deduction of concentration based on the colour intensity of the dye solution at constant time intervals. Absorption measurements at 665nm were taken every 15 minutes for the MB solution. These were then compared to an absorption-concentration calibration curve generated using standard solutions to obtain concentration values. A pseudo first order reaction rate was assumed. Hence, graphs of Ln C_o (Av)/C were plotted to obtain degradation rate constants, k. Values of k and of the final data points were compared to each other during analyses as a measured of the photocatalytic degradation efficiency observed.

In conclusion, the photocatalytic degradation efficiency increases with decreasing volumes, increasing incident light intensity at the correct wavelength, sufficient oxygen and mixing as well as increasing catalyst surface area; all of which are in line with literature. Evaporation was a significant factor identified in our experiments and a correction factor was needed for the other results due to it. However, this should not be a problem in real life applications, as the groundwater reservoir volume is large compared to the volume of water lost. The layered reactor design should also work well despite sacrificing light intensity on the further glass plates, as seen in the layer test series conducted. However, further scale model tests would still need to be done to ascertain and confirm its effectiveness.

Table of Contents

1 INTRODUCTION

1.1 Groundwater Pollution and Pollutants

For years, society has been single minded and relentless in its pursuit towards economic progress and increasing prosperity. More often than not, these activities have been at the expense of the environment; and our groundwater sources have not been exempt. With ~10,000,000 km^3 of the Earth's water stored in underground aquifers, groundwater makes up almost 98% of all unfrozen freshwater (Griffiths and Zabey, 2009). Rapid expansion of groundwater exploitation since the 1950s also means that ~50% of all drinking water, ~40% of industrial water and ~20% of irrigation water now comes from groundwater sources (Griffiths and Zabey, 2009). Unfortunately, this important water source is also one of the easiest to be polluted. And since they are out of sight, groundwater pollution very often goes undetected. But what can be said is that groundwater contamination is almost always the result of human activity (US EPA, 1993 adaptation).

Groundwater pollution is usually classified by its origin, with the four most common sources being: municipal, agricultural, industrial and individual. Contaminants can either be organic or inorganic substances. But since large quantities of organic compounds are manufactured and used by industry as well as in agricultural and municipal applications daily, these man made organic compounds are of most interest where clean-up is concerned (Lenntech, accessed May 2012). Thus, groundwater clean-up, especially of water soluble organic pollutants (eg MTBE), is not an option but rather a necessity.

Sadly, treating this precious resource is very difficult, even more so than other water sources since access to it is complicated. As a result, existing groundwater remediation technologies are often either inefficient, expensive or involve the introduction of additional consumable chemical reagents which can be hard to control (Chan, 2005). The use of multiple remediation technologies for a single clean-up process plus ex-situ procedures (Lim, 2010) also show current systems to be complex yet inconclusive. Thus, there is great need for a clean and cost-effective in-situ groundwater clean-up technology that works.

1.2 Existing Groundwater Treatment Technologies

MTBE, the organic pollutant of concern in our research, is the second most frequently found chemical in shallow ambient groundwater samples from urban areas (Deeb et al, 2000; Sahle-Demessie et al, 2002) despite elimination from consumption in the US in 2006.

This issue of cleaning up MTBE is even more prevalent as it is also highly water soluble, mobile and has low Henry's Law constant, thus making it especially persistent (Lim, 2010).

Technologies used to remove pollutants such as MTBE can generally be categorized as ex-situ or in-situ remediation. But most are ex-situ except bioremediation, phytoremediation and chemical oxidation (Lim, 2010). Current treatment technologies are:

a) Air Stripping

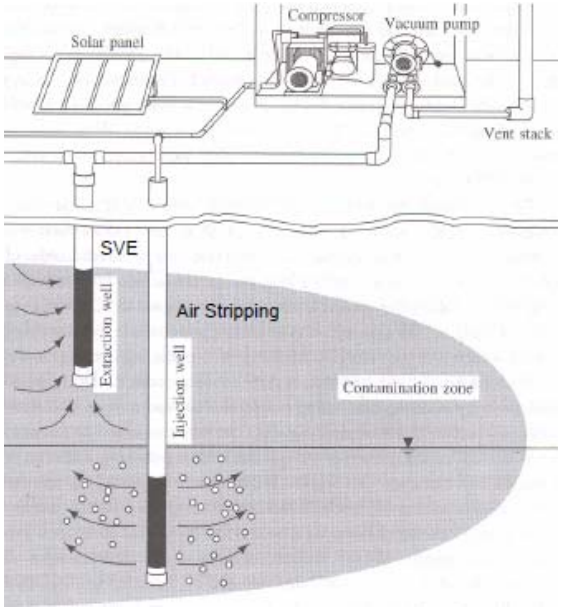

Figure 1: Coupling of air stripping (right) and SVE (left) in a groundwater remediation project (Fetter, 1999)

This liquid to gas transfer process involves injecting air into polluted groundwater to vaporise volatile organic compounds (VOC). Dissolved VOCs partition to the injected air based on their Henry's Law constant (HLC), which governs the natural tendency for organics to volatize from aqueous to gas phase (Chan, 2005). Thus, lower HLC pollutants (such as MTBE) would need a higher airflow. Although relatively simple to implement as it only involves a physical process, it can be very energy intensive for contaminants with low HLC (Lim, 2010). Additionally, air stripping also does not destroy the organic pollutants but simply transfers them from water to air, requiring extra clean-up technologies for full remediation and thus increasing project costs.

b) Multiphase Extraction (MPE) and Soil Vapour Extraction (SVE)

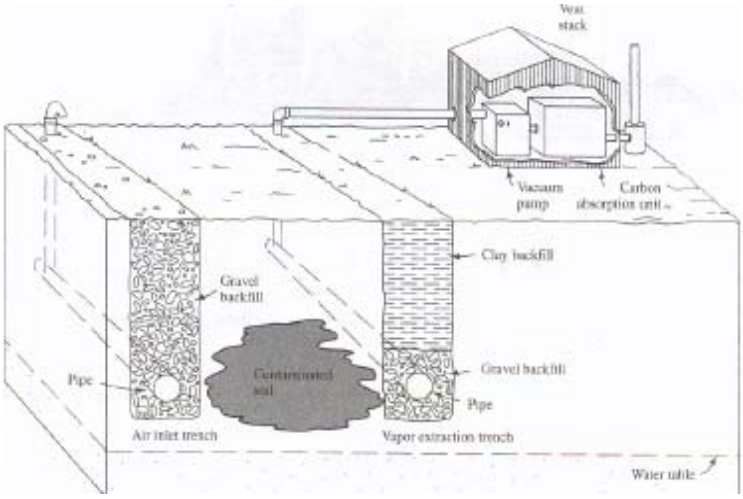

Figure 2: Soil Vapour Extraction (SVE) System (Fetter, 1999)

Multiphase Extraction (MPE) technologies such as Soil Vapour Extraction (SVE) involve the simultaneous extraction of soil vapour and groundwater to remediate both types of contaminated media (US EPA, 1999). It is among the most popular remediation technologies, applied in 42% of

remediation projects in the US (US EPA, 2004) but is usually used to control contaminant spread rather than cleaning it up (Lim, 2010). It works best for volatile contaminants or in conjunction with air stripping to enhance removal (Lim, 2010). But similar to air stripping, MPE also does not actually destroy the contaminants but require combinations with other above ground (ex-situ) technologies for full remediation.

c) Bioremediation

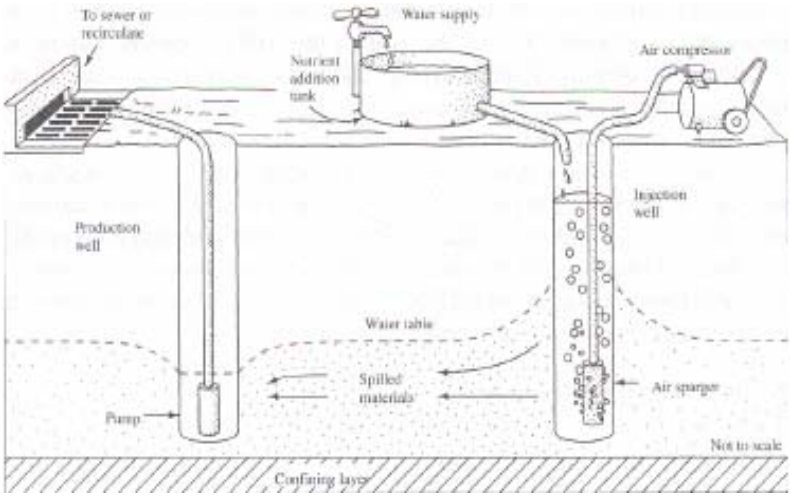

Figure 3: In-situ Bioremediation (Fetter, 1999)

Bioremediation works by enhancing the natural biodegradation process of organic contaminants by stimulating microbial activities through the supply of air, nutrients etc. (Lim, 2010). Unlike air stripping or MPE, it can work both ex-situ (bioreactors) and in-situ (permeable barriers), often in a standalone system (US EPA, 2004). However, it is highly dependent on the type of pollutants and bacteria used as the presence of other pollutants may inhibit the biodegradation of the interested pollutant due to microbe selectivity. Aeration is also particularly important here to obtain aerobic rather than anaerobic biodegradation, as it is faster and less toxic. Bioremediation is safe and environmentally friendly, albeit slower than other procedures (Lim, 2010).

d) Advanced Oxidation Processes (AOP)

Figure 4: In-situ Chemical Oxidation (ISCO) Project (Reference)

Advanced oxidation processes (AOP) used for groundwater remediation often involve the introduction of chemical oxidants such as hydrogen peroxide into the subsurface. A rapid and mildly selective process, it can degrade many inert contaminants not affected by bioremediation (Lim, 2010), frequently in standalone systems (US EPA, 2004). However, many health and safety issues are associated with the ISCO method namely with regards to the handling and controllability of the chemicals injected as well as the off-gas that may

result (US EPA, 2004) since full retrieval of the introduced chemicals or their side effects on the groundwater components cannot be guaranteed. Photocatalysis is another type of AOP focusing on using immobilised catalysts instead.

e) Pump and Treat

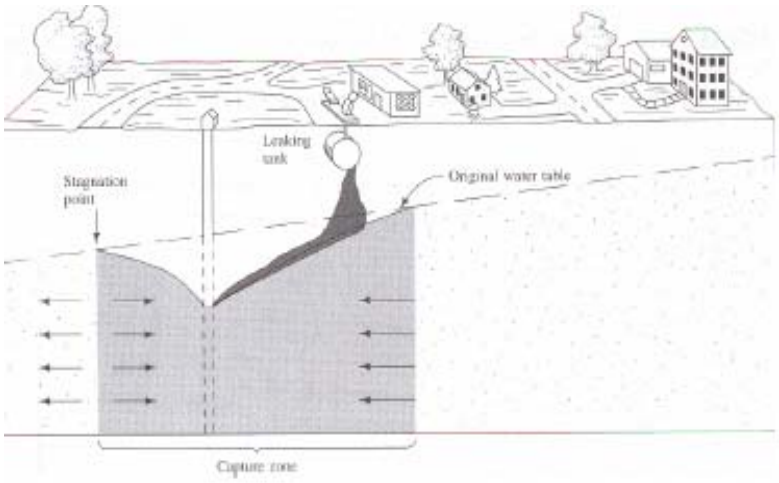

Figure 5: Groundwater Extraction using a Pump and Treat System (Fetter, 1999)

The pump and treat method is similar to SVE except that the withdrawal of contaminants is in the form of groundwater. Therefore, similar to SVE, pump and treat systems are more suitable for contaminant migration control instead of groundwater remediation as it could not completely remove contaminants (Mackay and Cherry, 1989). It is also usually coupled with above-ground treatment technologies. Thus, pump and treat systems generally require higher costs and longer project times (US EPA, 2004). But removal efficiency can be enhanced with isolation barriers or wells (Domenico and Schwartz, 1997).

f) Adsorption

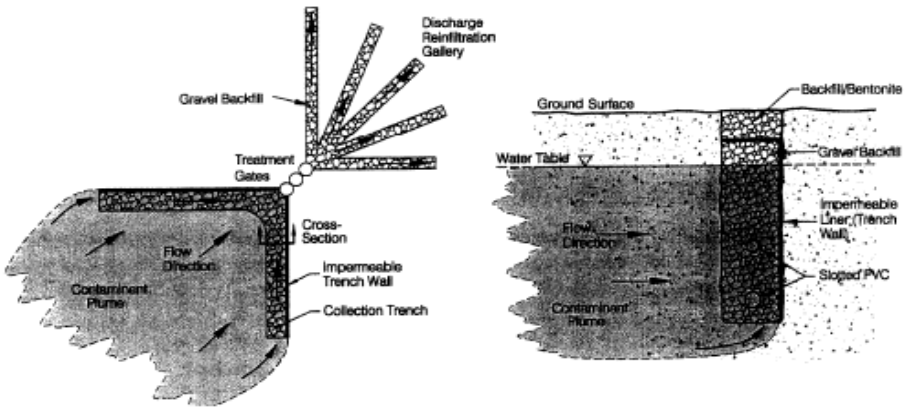

Figure 6: Funnel and Gate (left) and Trench (right) Systems (Bowles et al, 2000)

Adsorption is a physiochemical process involving the adhesion of contaminant molecules to a surface and is commonly seen in the form of barriers in trenches and funnel gate systems as seen in Figure 6 (Lim, 2010). However, the contaminants are not degraded, but simply transferred to the solid medium. Efficiency is affected by contaminant adsorptivity (low for MTBE), adsorbent porosity and the presence of more strongly adsorbed constituents. Adsorption processes are expensive to operate and changing environmental regulations indicate it may soon be prohibited (Chan, 2005).

1.3 Photocatalysis and Photocatalytic Reactors

As seen in section 1.2, though effective, current groundwater clean-up technologies present significant drawbacks. In particular, ex-situ processes are more expensive and complex as they typically involve a combination of technologies (Lim, 2010). There are also regulatory concerns since, according to the Water Framework Directive (European Commission, 2000 and 2006), water is not allowed to be extracted, partially treated and recharged back into the ground. In-situ techniques such as ISCO on the other hand, involve the injection of additional chemical oxidants to combat the pollutants, leading to health, safety and controllability issues. Many of the currently employed techniques also do not actually decompose the pollutants but only transfer them to another medium.

Photocatalysis, an AOP effective in degrading a plethora of compounds (Hoffmann et al, 1995; Hermann, 2005), provides a promising new alternative in-situ remediation technique using a non-toxic, immobilised catalyst that can be regenerated (thus creating less waste) using relatively simple equipment (Lim, 2010). Full photocatalytic oxidation also only produces water, carbon dioxide and simple mineral acids (Mills et al, 1993; Hoffmann et al, 1995; Barreto et al, 1995). The reaction (except initial adsorption) will only be initiated when UVA light is illuminated on the catalyst with no additional chemical oxidants required (Chan and Lynch, 2003a and b), thus making it a controllable and localised treatment (Chan, 2005). However, the process does require a relatively longer clean-up time, but since groundwater flow is significantly slower than wastewater treatment flow, sufficient clean-up time can be achieved; although some extra mixing and aeration to stimulate the reaction further may be needed. Large scale deployment also remains as yet, untested.

There are two main types of photocatalytic reactor designs proposed, mostly for wastewater treatment: slurry reactors and immobilised catalyst reactors. In slurry reactors, the TiO_2 powder is suspended in the water, giving higher photocatalytic activity due to higher catalyst surface area. However, post-treatment solid-liquid separation of the TiO_2 nanoparticles which is costly and technically complicated to implement would be needed (Balasubramanian et al, 2004). Therefore, should slurry reactors be implemented for groundwater treatment, it would have to be used ex-situ as part of a pump and treat system. Hence, immobilised catalyst reactor designs that have the TiO_2 powder fixed to a support are preferred for more cost effective in-situ treatment. Currently proposed slurry reactor designs include the Fountain Photocatalytic Reactor (Li Puma and Yue, 2001), Falling

Film Reactor (Almquist et al, 2003) and the Solar Parabolic Photocatalytic Reactor, which has had several variations of the design concept developed to a larger scale (Alfano et al, 2000; Robert and Malato, 2002; Mehos and Turchi, 1993; Bahnemann, 2004). While the proposed immobilised catalyst reactor designs are the Optical Fibre Reactor (OFR) (Peil and Hoffmann, 2000), Multiple Tube Reactor (MTR) (Ray and Beenackers, 1998a), Rotating Disk Photocatalytic Reactor (RDPR) (Dionysious et al, 2000b), Photocat I (Chan et al, 2006) and Honeycomb I (Lim, 2010). Of these designs, only Photocat I and Honeycomb I from previous departmental research work were specially designed for groundwater treatment.

1.4 Previous Research

This project follows from the PhD research of Chan (2005) and Lim (2010) plus ERASMUS project student Lusci Maria Elena on the remediation of MTBE using photocatalysis. The proposed honeycomb (Lim, 2010) and cylindrical (Chan, 2005) design configurations both used self-manufactured P25 TiO_2 coated mesh catalysts. In recent literature however, the main applications of photocatalysis were reported in wastewater clean-up and self-cleaning window glass, which has served as our research inspiration.

1.5 Aims and Objectives

The aim of this project is to explore the possibility and test the effectiveness of commercially available ActivGlass self-cleaning window glass for the photocatalytic clean-up of groundwater. Unlike the mesh catalyst used previously, ActivGlass is commercially available; thus the self-manufacture of the immobilised TiO_2 catalyst would not be needed, saving both time and money. Following that, the project also aims to establish the limiting factors of the reaction and use the information gathered during these tests to propose a design configuration that maximises pollutant removal, which needs to be tested further.

2 THEORY AND LITERATURE REVIEW

2.1 The Photocatalytic Mechanism

In general, photocatalysis can be described as the degradation of compounds in the presence of a photocatalyst, oxygen and appropriate light (Chan, 2005). It can occur in both aqueous and vapour conditions at room temperature; and unlike some of the other in-situ clean-up methods, it does not rely on high temperatures (AOP), additional oxidising agents

(ISCO) or bacteria (bioremediation). It was also found to be effective in degrading a plethora of organic compounds such as aliphatic alcohols, carboxylic acids, halogenated alkanes and alkenes, dyes etc. (Mills et al, 1993; Hoffmann et al, 1995). Plus, it was also proven to effectively break down inorganics like pesticides, insecticides and surfactants (Bhatkhande et al, 2001; Hermann, 2005; Mills et al, 2003).

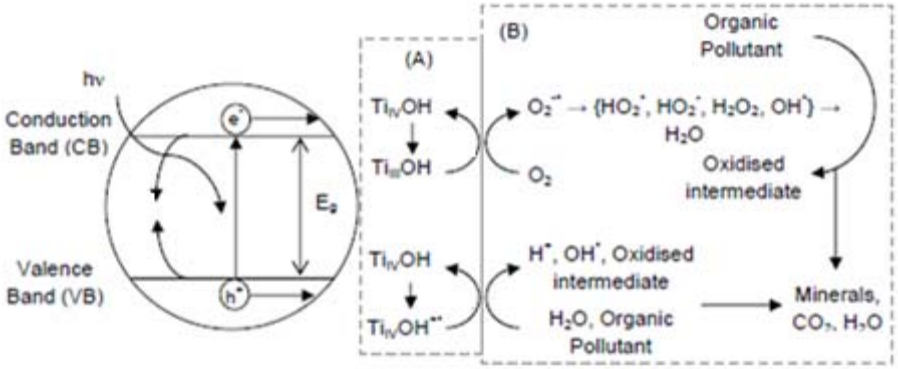

Figure 7: Primary Stages in Photocatalytic Mechanism (Lim, 2010 as modified from Hoffmann et al, 1995)

Figure 7 summarises the tree stages of the photocatalytic mechanism, which are:

a) Generation of electrons and holes

Irradiation of light induces photons of energy, $\mathbf{E_p = h\nu}$ onto the illuminated photocatalyst surface characterised by its band-gap energy, E_g; where h is the Planck's constant and v is the photon's frequency. If the photon energy, E_p is greater than the band-gap energy, E_g, electrons would be promoted from the semiconductor's Valence Band (VB) to its Conduction Band (CB). This in turn would generate a hole in the VB where the electron had left it. Both the VB hole and CB electron are highly reactive and can react with electron donors/acceptors respectively. However, recombination of these charge carriers can occur in the absence of suitable electron/hole scavengers, releasing heat. Thus, care should be given to ensure oxygen and water are in excess so that input light energy is not wasted. The wavelength of light required can be determined using the Planck's equation: Wavelength, $\mathbf{\lambda = hc/E_p}$, where h is the Planck's constant and c is the speed of light. Since catalyst activation will only occur when $\mathbf{E_p \geq E_g}$, the wavelengths for activation would therefore be $\mathbf{\lambda \leq hc/E_g}$. For the TiO_2 catalyst, E_g is roughly 3.1eV, giving λ_{max} ~ 400nm.

b) Formation of hydroxyl radicals

On the catalyst surface, water molecules are adsorbed and capture the VB holes to form highly reactive hydroxyl radicals (OH**.**) and hydrogen ions (H^+). Dissolved oxygen molecules are also adsorbed onto the catalyst surface but capture the extra CB electrons instead to

form oxygen radicals (O_2^-.). These oxygen radicals then further react with the hydrogen ions to first form hydrogen peroxide (H_2O_2) and then finally more hydroxyl radicals. Unlike the CB electrons (e_{CB}^-) and VB holes (h_{VB}^+), the hydroxyl radicals are not immobilised by the catalyst but are free to move within the aqueous solution, increasing the degradation effectiveness.

c) Degradation of pollutant molecules

The degradation of pollutant molecules, R, can occur indirectly via the free hydroxyl molecules or directly via the e_{CB}^- or h_{VB}^+ according to the equations below (Chan, 2005):

Indirect oxidation: $OH. + R \rightarrow R' \rightarrow CO_2 + H_2O + R''$

Direct oxidation: $h_{VB}^+ + R \rightarrow R' \rightarrow CO_2 + H_2O + R''$

Direct reduction: $e_{CB}^- + R \rightarrow R' \rightarrow CO_2 + H_2O + R''$

The exact reaction pathways differ for different pollutants, but for full degradation, the final products would be CO_2 and H_2O (and simple mineral acids) only for all contaminants (Chan, 2005). Recombination can occur here too if pollutants are insufficient.

Kinetically, photocatalysis is a pseudo first order reaction under no flow conditions and the efficiency of degradation can be measured concisely by the rate constant, k such that: **$C = C_o \exp(-kt)$** and hence **$kt = \ln(C_o/C)$** as seen in Figure 8 below (Chan, 2005).

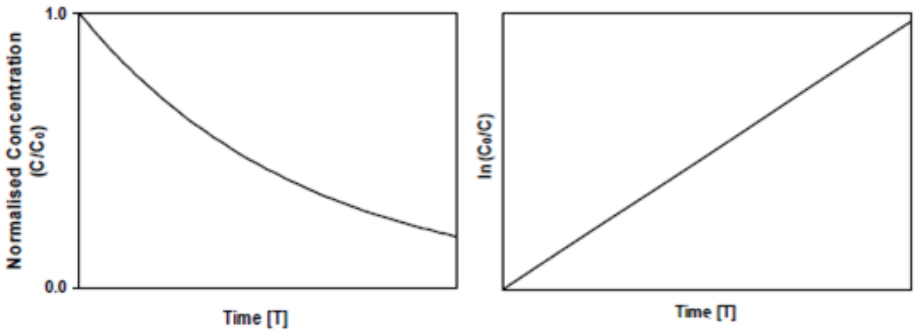

Figure 8: (left) Typical exponential decay curve of a contaminant (right) Typical linear plot of $\ln(C_o/C)$ vs time

2.2 The TiO_2 Catalyst

A catalyst is a chemical that activates a reaction which will not happen spontaneously otherwise, and remains unchanged and unconsumed at the end of the reaction (Chan, 2005). Photocatalysts specifically, are semiconductors like TiO_2, ZnO or Fe_2O_3. (Mills et al, 1993) characterised by their distinctive band-gap energies, similar to resonant frequencies. TiO_2, an n-type semiconductor widely used in photocatalysis, is preferred as it is non-toxic, photostable, commercially available, cheap and catalytically efficient (Alfano et al, 1997).

Mills et al (1993) also further showed TiO_2 to be the most active among the other semiconductor photocatalysts tested (ZnO, WO_3, CdS and SnO_2) in degrading a range of organic contaminants. The use of TiO_2 as a photocatalyst is even more cost effective because it also remains intact before and after treatment contributing to a longer lifespan compared to ISCO (Mills et al, 1993; Hoffmann et al, 1995). Furthermore, it can be recycled with no significant reduction in photocatalytic activity (Bhatkhande et al, 2001; Mills et al, 1993). But the main benefit in using TiO_2 for groundwater clean-up is its manageability and safety. TiO_2 is a non-toxic, biologically and chemically inert material, needing no special health and safety measures for handling (Mills et al, 1993; Hoffmann et al, 1995). The process is also highly controllable since the reaction (except some adsorption), will cease once the UV light is switched off due to TiO2's relatively high band-gap energy (Mills et al, 2003). Unfortunately, this also means the major cost component of a photocatalytic reactor is in the energy consumption of the UVA artificial light source. This is the major shortcoming for rapid commercialisation of photocatalytic water treatment (Bahnemann, 2004).

Physically, TiO_2 appears as a white, insoluble solid at room temperature, consisting 60% Ti and 40% O (Lim, 2010). Commercially available TiO_2 usually exists in 2 different crystalline microstructures: rutile and anatase (Brown et al, 1999). The amorphous phase of TiO_2 is not photocatalytically active (Lim, 2010). Extensive examination of the properties of both these microstructures by Won et al (2001) showed that the anatase form is photocatalytically more active in degrading organics, possibly due to its higher electron transfer rate and specific surface area (Hoffmann et al, 1995; Bhatkhande et al, 2001). However, the anatase form also has a higher electron-hole recombination rate (Ryu and Choi, 2008). Therefore, the presence of some rutile TiO_2 is necessary to minimise this phenomena and increase performance (Hoffmann et al, 1995). Additionally, the rutile phase is also more effective in photocatalytically degrading inorganic chemical compounds and could perform better on certain chemicals like methanol and Methylene Blue dye (Ryu and Choi, 2008). Hence, typical commercially available TiO_2, Degussa P25, consist of 20-30% rutile and 70-80% anatase (Mills et al, 1993; Bhatkhande et al, 2001).

Previous departmental research by Chan (2005) and Lim (2010) aimed to modify and immobilise this TiO_2 powder catalyst for use in immobilised photocatalytic reactors. In order to compare the photodegradation effectiveness of ActivGlass self-cleaning glass, this project used the P25 TiO_2 mesh catalyst manufactured by Lim (2010) as a reference film catalyst.

2.3 Properties of ActivGlass Self Cleaning Window Glass

Semiconductor photocatalysis research has increasingly moved away from the powder forms of P25 TiO_2 to film coatings (Mills et al, 2003). However, immobilisation of the TiO_2 coating has proven tricky as films made from the P25 formula do not adhere well to surfaces, are not chemically stable or highly reproducible (Mills et al, 2003). Pilkington ActivGlass, comprising an active film layer of nanocrystalline TiO_2 ~15nm thick, is a suitable successor to the P25 as a benchmark for film photocatalysis comparisons (Mills et al, 2003).

ActivGlass is made from 4mm float glass with a clear, colourless, effectively invisible photocatalytic coating of TiO_2 (Mills et al, 2003) deposited using an Atmospheric Pressure Chemical Vapour Deposition technique (APCVD) on one side. It uses the photocatalytic oxidation (PCO) and photo-induced superhydrophilicity (PSH) properties of TiO_2 to remove pollutants adsorbed onto its surface (Chin and Ollis, 2007). ActivGlass has a haze of less than 1%, reflectivity of 5-7% and reduces levels of solar UV light transmitted through it by 20% (Mills et al, 2003). It is also extremely robust mechanically (Pilkington website), which is its main advantage over the more active P25 films (Mills et al, 2003).

In tests to determine the light driven kinetics of ActivGlass in air, it took ~850-1200min to achieve 90% dye decolorization with 365nm irradiation while 95% decolorization was possible within just 480min under solar conditions (Chin and Ollis, 2007). This higher reaction rate was attributed mainly to the presence of extra UVB photons which can also activate the TiO_2 catalyst (Chin and Ollis, 2007). This was further confirmed by Mills et al (2003) when ActivGlass efficiency was tested for stearic acid degradation under 365nm and 254nm light; showing marked increase in the initial rate and formal quantum efficiency of ActivGlass with the latter because of the greater absorption coefficient of TiO_2. Humidity, mass loading, oxygen content and PSH can also affect the degradation efficiency of ActivGlass. Mills et al (2003) found that the photocatalytic degradation rate is 3 times slower at 0% humidity due to insufficient hydroxyl radicals produced (Chin and Ollis, 2007). While time needed for 90% dye decolorization was 10 times greater for thick multilayers as there is more dye to absorb more of the incident UV light (9-20%), decreasing the number of photons reaching the TiO_2 layer (Chin and Ollis, 2007). But as time progresses, the dye layer decreases, so more photons can reach the TiO_2 film. Additionally, degradation simply does not occur without oxygen and PSH increases contact of pollutant and catalyst surface by spreading it, increasing degradation efficiency (Mills et al, 2003; Chin and Ollis, 2007).

2.4 Use of Methylene Blue (MB) Dye

Common dyes like MB are often used to assess the principles of photocatalysis and activity of photocatalysts, both under vapour or aqueous phases (Mills et al, 1993; Ryu and Choi, 2008). Similarly, MB was used as a proxy for MTBE to measure the effectiveness of ActivGlass for the remediation of MTBE in groundwater in this project.

MB is a basic aniline dye which appears as a solid, odourless dark green powder at room temperature and yields a blue solution when dissolved in water, giving a well-defined optical absorbance maximum at 660-665nm (Lim, 2010). But when exposed to a reducing agent, the dye decolorizes, turning colourless (Lim, 2010). Hence, by measuring the colour concentration of the MB solution at regular time intervals (Mills et al, 1993), the degradation efficiency rate of the photocatalyst tested could be obtained easily (much easier compared to measuring concentration of MTBE directly). The photocatalytic degradation pathway for MB dye is as in Figure 9 (Houas et al, 2001). Intermediate products were proposed here based on molecular weight but the final products will only be water and carbon dioxide (Houas et al, 2001). Since MB decolourisation is prompt (Houas et al, 2001), we can assume a single step procedure without coloured intermediates, which would greatly simplify our analysis.

However, once we have established a list of limiting factors for the ActivGlass oxidation reaction process, we can and should move on to using real pollutants for a more realistic view of using this technology for groundwater clean-up.

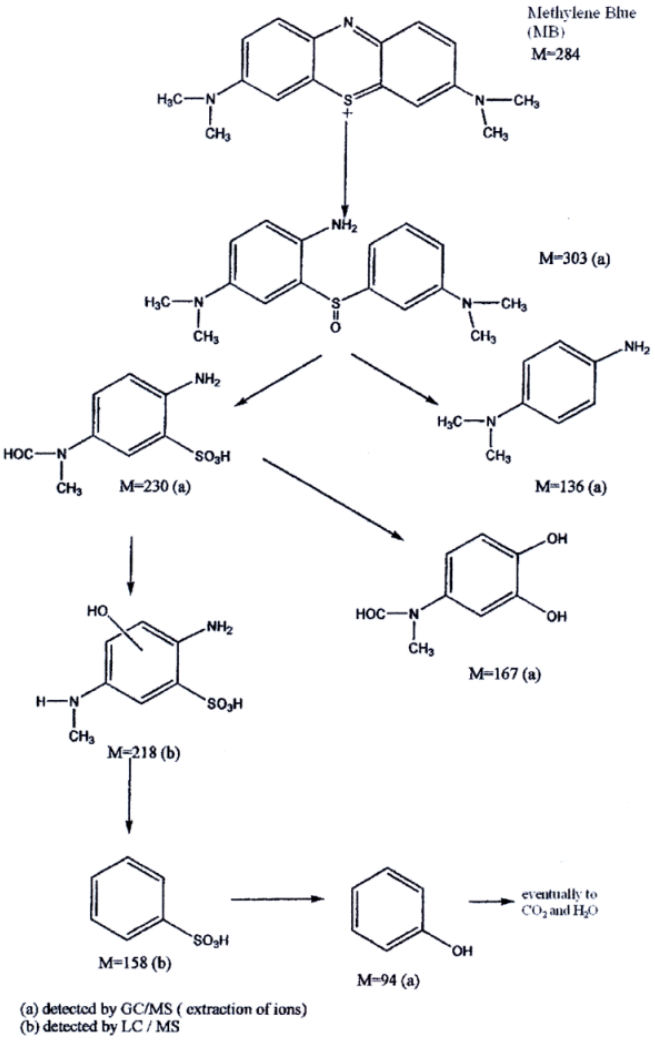

Figure 9: Proposed photocatalytic degradation pathway of Methylene Blue dye (Houas et al, 2001)

2.5 Assumptions and Theoretical Expectations

Literature has shown extensively the factors that could affect the degradation efficiency of a photocatalyst and our research aims to test some of these on ActivGlass:

a) Oxygen (Aeration)

From Section 2.1, it is clear that Oxygen functions not only in the oxidation process but is essential in preventing the recombination of electrons and holes too (Chan, 2005). Thus it follows that higher oxygen content would result in a higher degradation rate (Dionysiou et al, 2002). Additionally, aeration can also provide sufficient turbulence/mixing to ensure uniform concentration in the reactor (Lim and Lynch, 2010). Unfortunately, this can also vaporise the pollutants instead of cleaning it, similar to air stripping (Lim and Lynch, 2010). Hence, the effects of vaporisation should be accounted for whenever aeration is involved.

b) pH

Mills et al, 1993 showed that photocatalysis is not strongly dependent on pH with effects on efficiency of less than an order of magnitude. In fact, most literature reported constant degradation rates across different pH levels for various organic pollutants (Choi et al, 1997; Rideh et al, 1997; Davis and Green, 1999). Thus, pH adjustments were deemed unnecessary for photocatalytic reactors operated under ambient conditions (Agustina et al, 2005).

c) Temperature

Photocatalysis is light rather than heat activated (Hermann, 2005). In fact, below 70^{o}C, its effect on efficiency is small; but above 70^{o}C, the activation energy is negative and so the rate of adsorption of reactants is reduced, thus slowing down the photocatalytic process (Hermann, 1995). Since the lab temperature is controlled at 21^{o}C (increasing to ~29^{o}C with the use of the 15W lamp), the effect of temperature can be neglected. But the rate of vaporisation does increases with temperature even at ambient values (Lim, 2010).

d) Pollutant Concentration

The rate of photocatalytic degradation is proportional to the instantaneous concentration of pollutants (Chan, 2005). The light absorption spectrum of a pollutant has significant impact on the kinetics of photocatalysis, with degradation rate varying inversely with the concentration of strong UV absorbers as they will screen the catalyst from the light source (Mills et al, 1993). This is however unlikely to be significant for organic pollutants such as MTBE as they do not absorb UV strongly (Mills et al, 1993). This issue of turbidity is an often overlooked major drawback for TiO_2 photocatalysis in water purification (Mills et al, 1993).

e) Surface Area and Adsorption

The number of active sites for the adsorption of compounds, and hence photocatalytic reaction, is proportional to the catalyst's specific surface area (varies inversely with particle size) (Lim, 2010). This can occur even in the absence of UV light and its effects were analysed in the initial hour of our tank reactor tests. But for low adsorptivity pollutants (eg MTBE), the effect of adsorption is negligible as most of the degradation is via more mobile hydroxyl radicals off the catalyst surface (Ryu and Choi, 2008).

f) Presence of Other Pollutants

The presence of competitive adsorbents would challenge and inhibit the overall reaction rate due to the deactivation of reactive sites (Lim, 2010). Molecules that adsorb more strongly will degrade preferentially, inhibiting the subsequent adsorption of other molecules onto the catalyst surface (Sahle-Demessie et al, 2002b). The competition for hydroxyl radicals amongst the molecules would also increase, further reducing the removal rate of a target contaminant (Matthews, 1992). Thus, rate constants of pollutants in mixtures are always smaller than that of the pollutant alone (Chan, 2005).

g) Light Intensity and Wavelength

Section 2.1 also detailed the importance of appropriate light wavelength in the photogeneration of hydroxyl radicals and other charge carriers crucial for the redox reactions. The efficiency of the reaction also generally increases with input light irradiance and intensity (Chan, 2005). Studies by Hermann (2005) and Mills et al (1993) further showed that the proportionality of the photocatalytic reaction rate changes from I to $I^{0.5}$ at light intensity above ~25mWcm^{-2} (high intensity).

h) Volume of Solution to Clean Up

Ray and Beenackers (1998) and Chen et al (2001) clearly showed that the rate of photocatalytic degradation increased with A/V, where A is the catalyst surface and V is the volume of the reactor. This means that in terms of volume to clean up under constant catalyst area, a higher degradation rate would be achieved with lower solution volumes.

In our research experiments below, we have assumed that the general relationships and trends between these factors and the degradation efficiency hold. Our tests aim to further investigate how these factors affect the ActivGlass degradation efficiency specifically. The identified factors discussed here to be investigated experimentally further in this project are: volume, light intensity, surface area, adsorption and oxygen/aeration.

3 EXPERIMENTAL DESIGN, TECHNIQUES AND APPARATUS

3.1 Experimental Setup, Conditions and Apparatus

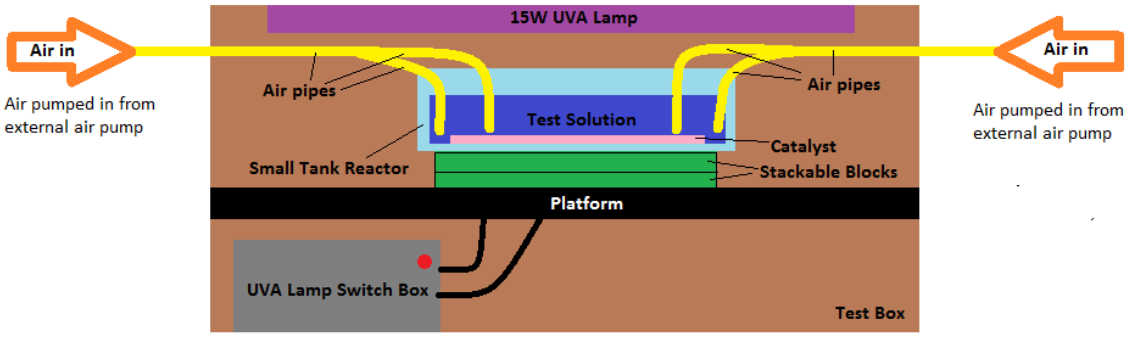

Figure 10: Experimental Setup

Figure 10 above shows the experimental setup used to test the degradation efficiency of ActivGlass under different initial conditions to assess how it changes with the factors highlighted in Section 2.5. This setup was inherited from the one used by ERASMUS student, Elena (2011) since it worked well when testing the limiting factors of Lim's (2010) self-manufactured mesh catalyst. From the diagram, it is clear that the setup consists mainly of a rectangular small tank reactor and a 15W UVA lamp concealed within a wooden box to reduce the effect of the environment (additional lighting), maintain constant temperature and to shield the user from harmful UV rays. The small tank reactor is a home-made Perspex vessel with dimensions 24cm x 10cm x 6.5cm. The samples of ActiveGlass and mesh catalyst were each cut to 21cm x 9cm pieces to fit into the reactor and enable testing. These catalyst samples were placed directly onto the base of the reactor with the MB test solution poured over it. On the other hand, the light source used is a 15W, 365nm Philips Cleo UVA lamp set directly above the small tank reactor, illuminating the catalyst samples. The distance between the catalyst and light source can be varied using a system of stackable blocks placed beneath the vessel. The combined thickness of the blocks can range from 0mm (no blocks) to 50mm (two 20mm blocks and one 10mm block). Additionally, the aeration and mixing conditions were controlled by an external Hagen A-807 Optima air pump, directing air into the four corners of the vessel via thin air pipes fixed in position using binder clips ~5mm from the catalyst surface to reduce turbulence within the vessel and to homogenise the oxygen dispersion into the water.

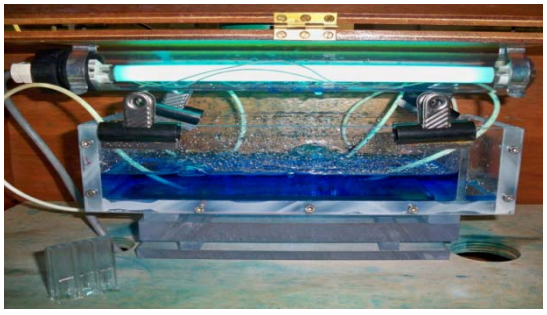

Figure 11: Small Reactor Tank Test in Progress

Figure 12 (left): Unicam 8620 UV/Visible Spectrophotometer

Figure 13 (right): Mettler AE160 Digital Balance

Other equipment used in this project include the Unicam 8620 UV/Visible spectrophotometer, Mettler AE160 digital balance and other measuring devices like pipettes and measuring cylinders. The spectrophotometer measures the absorbance of the liquid at a particular wavelength, which was then converted into a concentration value using a calibration curve. All absorption readings should be compared to a reference spectrum (water) to extract more meaning from them. Standard lab conditions (Temperature = 21^{o}C, low humidity) were maintained throughout the tests to ensure comparability. Temperature within the box can rise up to 29^{o}C when the UVA lamp is switched on.

3.2 Experimental Methods

3.2.1 Calibration

Prior to conducting the main experiments with the setup above, an absorption-calibration curve was plotted using a series of standard solutions, to enable conversion of the UV/Visible spectrophotometer absorption readings into concentration values.

100mg of MB hydrate solid was carefully weighed out on a scale before being diluted thoroughly in a conical flask with 1L of distilled water, giving a concentrated stock solution of 100mg/L. A stock solution was prepared because weighing trace amounts of MB hydrate solid accurately every time is very difficult, and a stock solution would be able to yield batches of test solutions with more similar initial concentrations. 10ml of this stock solution was then measured out using a measuring cylinder and poured into a beaker containing 90ml of distilled water to obtain the 10.00mg/L standard solution. Further dilution of this solution with equal parts water each time will yield standard solutions of 5.00mg/L, 2.50mg/L and 1.25mg/L. Solutions of other concentrations can be obtained similarly using the formula: $\mathbf{C_1V_1 = C_2V_2}$ where C_1 and C_2 are the concentrations of the stock and test solutions while V_1 and V_2 are the volumes of the stock and test solutions respectively. The

volume of water to be added for dilution, $\mathbf{V_w = V_2 - V_1}$. The absorptions at 665nm light for the 5 standard solutions were measured using the UV/Vis Spectrophotometer using pure water as a reference spectrum. A graph of Absorption against Concentration was the plotted and the slope of the linear region was obtained and used as the calibration constant. A further standard solution of 6mg/L was also created and its absorption measured to obtain a clearer picture of the transition area between the absorption for 5.00mg/L and 10.00mg/L concentration solutions to test the reliability of absorption readings in this range.

3.2.2 Small Tank Reactor Tests

Subsequently, a series of experiments were done using the setup in Figure 10, firstly to compare the reactiveness of Lim's (2010) manufactured mesh catalyst with the ActivGlass. Then, the reactivity of the ActivGlass under different initial conditions was analysed as well, including: varying test solution volumes, distance of the catalyst from the UV light source (light intensity), catalyst surface area, mixing and aeration.

A general procedure was followed for all the tests, varying only the initial configuration setup according to the factors tested. Firstly, the tank and ActivGlass/catalyst samples were cleaned and dried thoroughly using distilled water before being set up in the required configuration. Then, the stock solution prepared was diluted to 6mg/L (initial concentration for all tests) at the volume required and poured into the tank, covering the ActivGlass. The UVA lamp was switched off for the first hour to analyse the effects of adsorption alone, allowing it to reach equilibrium (Su et al, 2004). At the one hour mark, the UV lamp was switched on and kept on until the final reading at the 19^{th} hour. Typical experiments run for 19 hours each time including a 14 hour overnight period. Readings were taken every 15 minutes for the first 4 hours and then every half hour for the 5^{th} hour after which the tank was left overnight for 14 hours and a further reading was taken at the 19 hour mark. Readings were taken by obtaining 3 samples of the test solution in 4ml cuvettes using a pipette and then measuring their absorbance using the UNICAM 8620 UV/Vis Spectrophotometer at 665nm. The absorbance of this wavelength of light by distilled water was used as a reference. After the measurements were taken, the sample solutions were returned to maintain the volume of the test solution in the reactor. These readings were further recorded, and graphs of C/C_o (Av) against time as well as ln (C_o (Av)/C) against time were plotted. The ln curves were plotted because assuming a pseudo first order reaction

would yield a straight line for the degradation process. The gradient here, k gives a measure of the photocatalytic efficiency of the system. Finally, single pass overnight tests, where only the starting and ending measurements were taken, were also conducted as an extra check for the repeatability of the experiments and reliability of the results.

3.2.3 Other Tests

In addition to the calibration and main tank tests, other tests were also conducted namely to measure the transparency of the ActivGlass and MB dye at initial concentration towards light at 365nm (UV lamp wavelength) using the spectrophotometer. Using pure water as a reference again, the absorption of the small piece of ActivGlass and MB dye at 6mg/L in a 4ml cuvette were measured for a range of light wavelengths from 300-600nm for the glass and 305-705nm for the dye. This captured information on the transparency of both at 365nm and additionally for the dye, at 665nm too (corresponds to colour of dye).

Furthermore, the effects of evaporation were also analysed and the results used as a correction factor for the experimental measurements with aeration. Finally, configuration tests using multiple layers were also conducted to test the feasibility of our proposed layered reactor design using the information obtained from the reactor tank tests detailed previously. These tests were carried out in the same manner as detailed in Section 3.2.2.

Although literature of its performance in air suggests that the ActivGlass can be reused for a long time, a slight blue tinge was noticed after several uses in water with the dye. The transparency of the glass in this state was measured for 365nm but found to be just as good in allowing light of that wavelength pass despite the colouration, reaffirming the literature.

3.3 Experimental Accuracy

Experimental accuracy measures how close to a true or accepted value a measurement lies (points close to true value) while the precision of a result indicates how sharply it is defined and how closely the analytical results can be duplicated (points close together) (Lynch, 2012). Analysing the steps taken in our project, the main area of concern was identified to be in the weighing of MB hydrate solid, volume measurements, absorption readings and repeatability of the experiments when the ActivGlass catalyst was reused. The uncertainties for the various apparatus are:

- Mettler AE160 Digital Balance: ±0.1 mg
- Measuring Cylinder: ±1 ml
- Unicam 8620 UV/Visible Spectrophotometer: ±0.003 absorbance

This shows that the most inaccurate measuring apparatus used was the measuring cylinder. This is especially important when measuring out the stock solution to be diluted because very little goes a long way for the MB dye solution. When making the stock solution, it was also observed that very little of the MB hydrate solid was required and small changes that may not be picked up by the weighing scale actually made very big differences to the concentrations of the solutions made from it. This was why it was elected to produce a stock solution instead of weighing out the solid for dilution for each test (ensure similar initial concentrations). Thus, the sensitivity due to the digital balance was minimised. The spectrophotometer readings were presented digitally but it was observed that the readings sometimes fluctuated. Hence, a sensitivity of ±0.003 absorbance was introduced instead even if the spectrophotometer showed readings up to ±0.001 absorbance on screen. The repeatability of the experiments when the ActivGlass was reused was verified through single pass overnight tests detailed in Section 3.2.2.

Therefore, the overall uncertainty associated with the initial concentration value calculated is proportional to the concentration of stock solution based on the equation $\mathbf{C_1V_1 = C_2V_2}$ (volume ratio cancels out dependence), which in turn depends on the absorbance reading by the spectrophotometer, digital balance and measuring cylinder; thus giving **uncertainty = 0.1/10 + 1/1000 + 0.003/1.307 = 1.33%**

The instant uncertainty of subsequent concentration values however would only depend on the absorbance reading and measuring cylinder (dye and water volumes), giving:

Uncertainty = 0.003/local absorbance reading + 1/volume of dye + 1/volume of water

4 RESULTS AND DISCUSSION

4.1 Absorption-Concentration Calibration

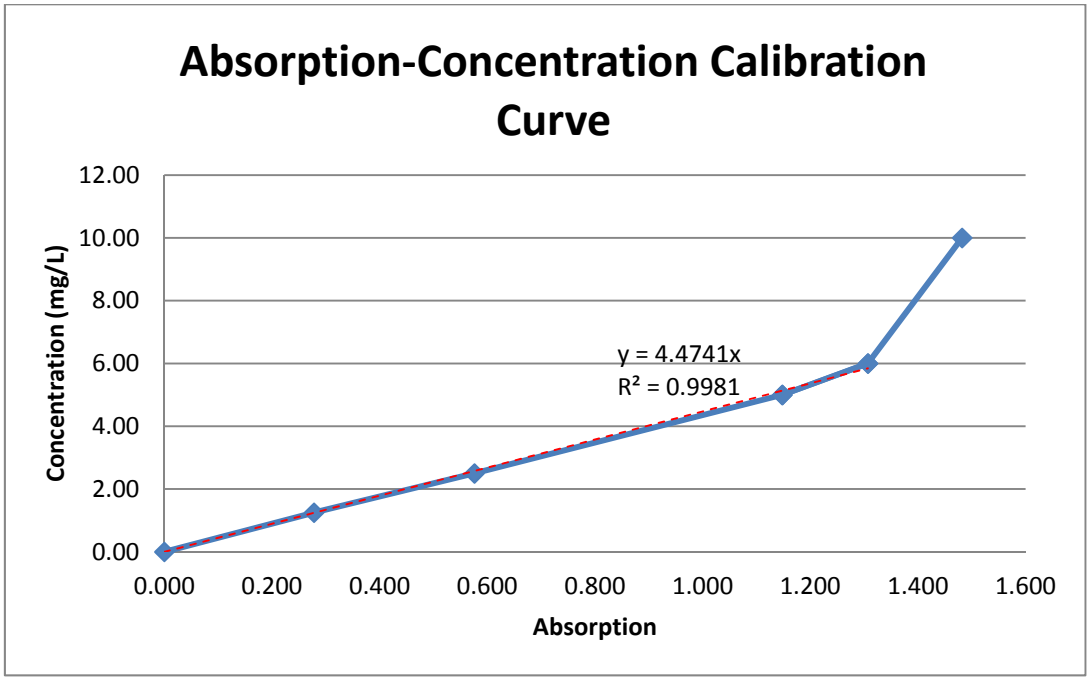

Figure 14: Absorption-Concentration Calibration Curve for Methylene Blue (MB) Dye

Figure 14 above shows the absorption-concentration calibration curve for MB dye at 665nm obtained according to the procedures outlined in Section 3.2.1. At low concentrations of up to about 7-8mg/L, concentration is directly proportional to absorption, in line with the Beer-Lambert Law which states that the absorbance, **$A = \log (I_o/I) = \log (1/T) = kcd$**. I is the transmitted light intensity, I_o is the incident light intensity, T is the light transmitted, c is the concentration, d is the path length travelled and k is the calibration constant since the cuvettes used had d = 1cm (Lynch, 2012 lecture notes). The Beer Lambert Law derives from the fact that light attenuates exponentially as it passes through clear materials or solutions. Thus, the transmittance would be exponentailly related to the concentration of a sample and the path length of light travelled.

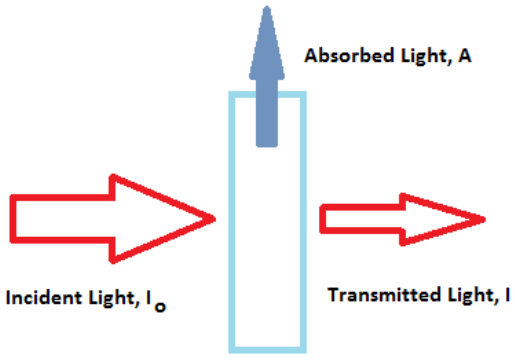

Figure 15: Schematic of Light Transmittance through a Medium according to Beer Lambert Law

The final data point on the absorption-calibration curve corresponding to 10mg/L concentration was rejected when trying to obtain a linear regression because an absorbance of ~1.5 is equal to ~97% light absorbed. At this point, the stray light performance of the instrument dominates, making the reading unreliable. The gradient of the curve in the linear region was then used in all subsequent experiments to convert the absorption readings taken into concentration values by the equation: concentration, **c = 4.4741 A** (absorbance).

4.2 UV/Visible Spectra

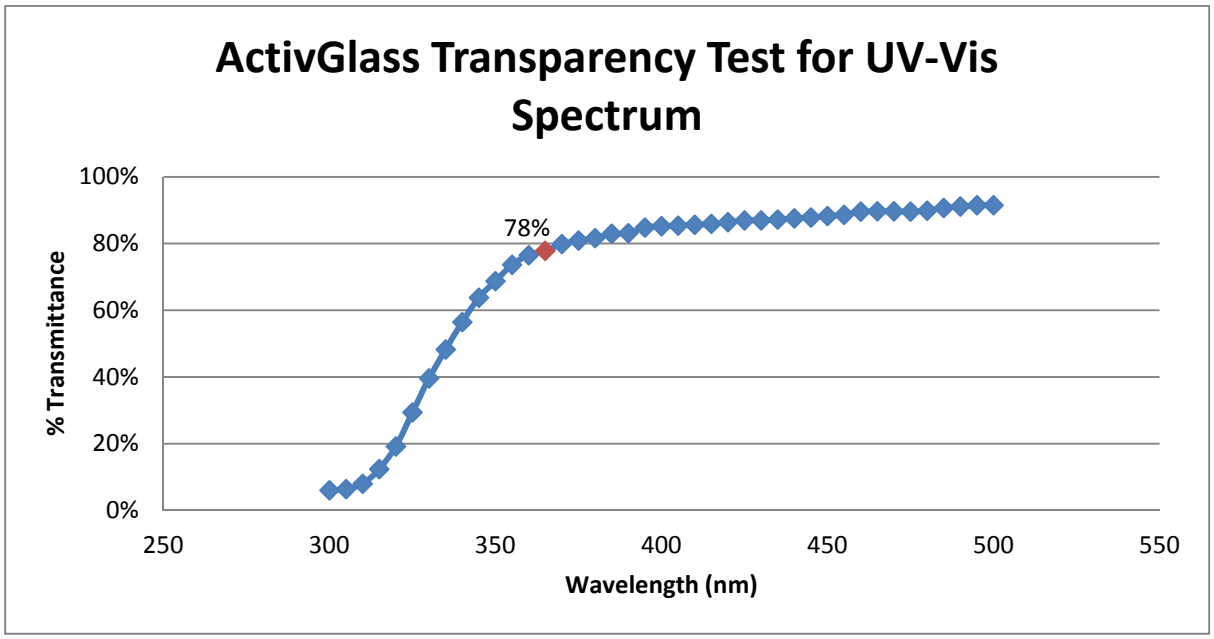

Figure 16: UV/Visible Spectrum of ActivGlass

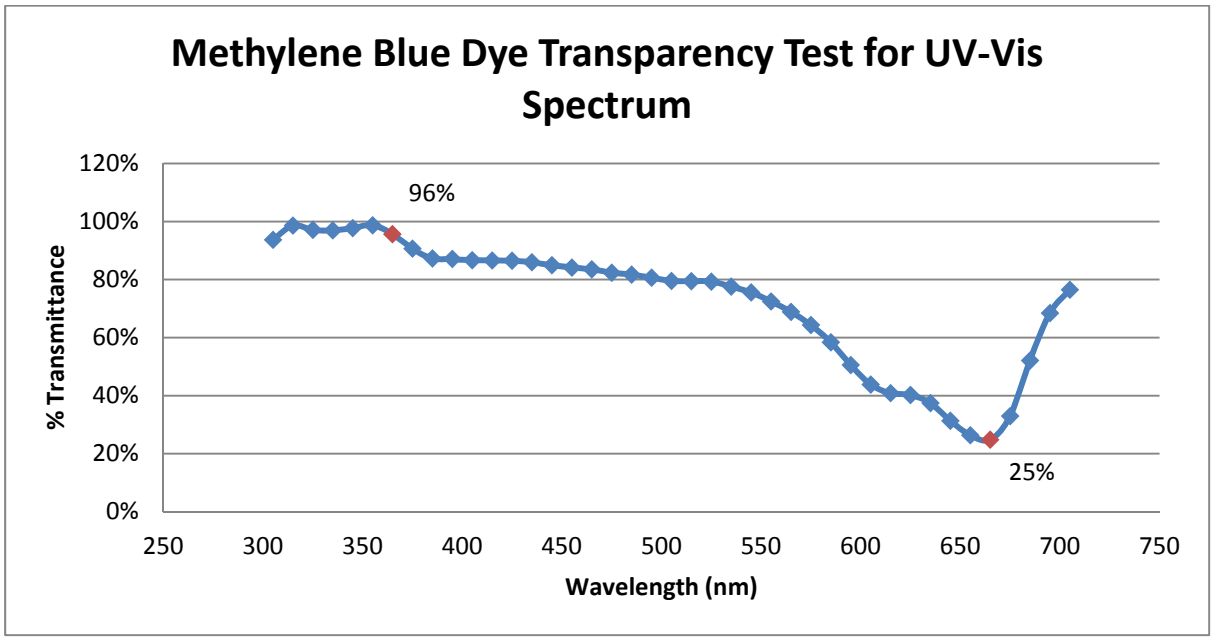

Figure 17: UV/Visible Spectrum of MB Dye at 6mg/L Concentration

Figures 16 and 17 show the UV/Vis spectra for ActivGlass and 1cm of MB dye at 6mg/L respectively. These tests were carried out to understand how much of the incident UVA light would be absorbed by the two mediums, and hence not reach the catalyst. It was hoped that this would assist in the design process for future equipment configurations.

From Figure 16, it is clear that 22% of UV light at 365nm will not pass through the glass (78% transmittance). However, this still presents a significant advantage over the mesh catalyst used before, which is opaque, as it now enables layers of the catalysts to be stacked close together and still be activated by a distant light source, increasing the flexibility and possibilities of design. However, care should be given to factor in the fact that light intensity would decrease by 22% after each layer in a layered design configuration.

Figure 17 on the other hand shows that the MB dye transmittance at 365nm is 96%, while at 665nm, it is 25%. This shows that the dye itself actually absorbs some of the UVA light too. Hence, if the pollutant/test solution is too concentrated or coloured (high turbidity), configurations with the catalyst below the light and solution (as in the experimental setup) may not work. However, this would be less relevant for pollutants with low absorbance at the incident light wavelength as the incident light would just pass right through it. Next, the dye also does not allow much light of wavelength 665nm to pass through it. In fact, it is the wavelength that gives minimum transmittance, corresponding with maximum reflectance, which is consistent with the solution showing a blue colour.

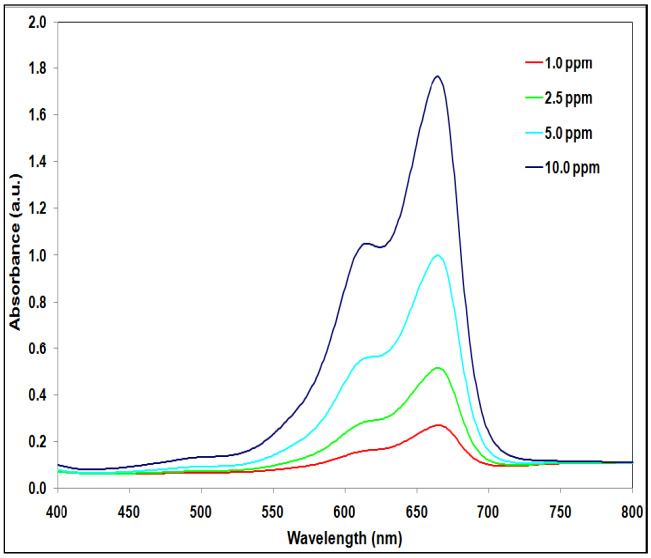

Figure 18: Absorbance Spectra of MB Solutions at Various Concentrations (Lim, 2010)

Figure 18 above further shows the absorbance spectra of MB solutions at various concentrations. Although the absorbance readings observed for lower concentration

solutions were also lower throughout, they all presented peak absorbance readings at roughly the same wavelength of 664nm (Lim, 2010). Other research showed similar results but at wavelengths of 660-665nm instead (Chan, 2005; Mills et al, 1993; Chang et al, 2006). Hence, taking readings at 665nm throughout the experiments (wavelength corresponding to lowest absorption based on Figure 17) even as the dye concentration drops with photocatalytic degradation is valid.

4.3 Standard TiO_2 Mesh-Glass Comparison

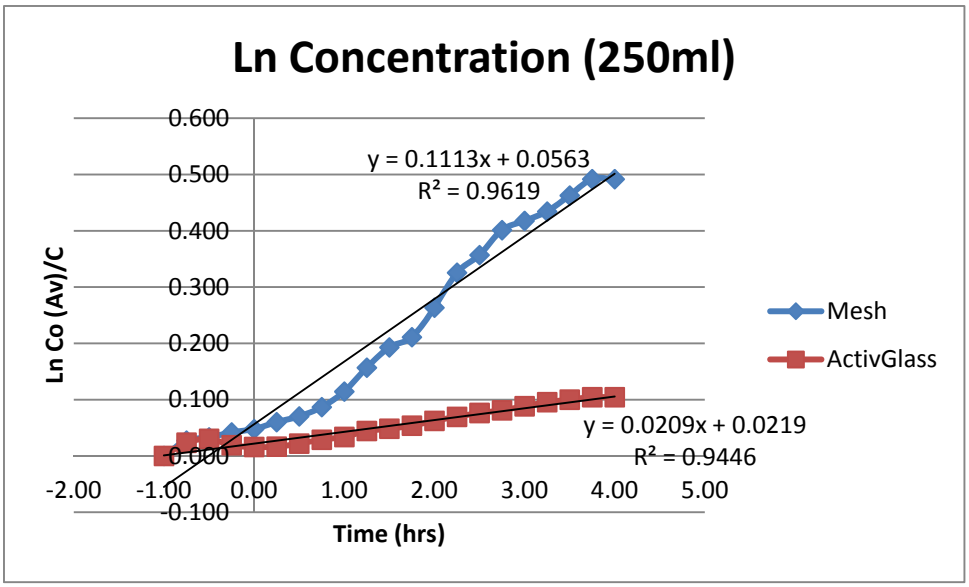

Figure 19: 5 hour Ln Concentration Curve for Mesh-ActivGlass Comparison

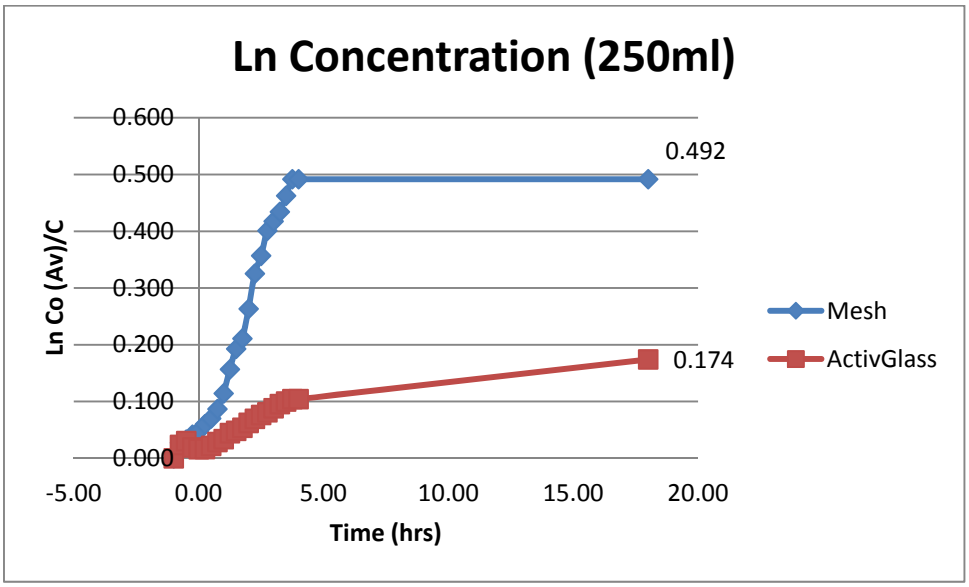

Figure 20: 19 hour Ln Concentration Curve for Mesh-ActivGlass Comparison

Figure 19 compares the reactiveness of the mesh catalyst and ActivGlass, showing the mesh catalyst to be roughly 5 times more reactive than ActivGlass (ratio of slopes).

Within a mere 5 hours, the mesh had cleaned up ~40% of the pollutants while ActivGlass only managed slightly less than 10%. However, when the experiment was extended for another 14 hours as in Figure 20, the reactiveness of the mesh starts tailing off as cleanup approaches its limit, thus allowing the ActivGlass to catch up, finally degrading to approximately 35% of what the mesh cleaned up. This indicates that it would take ~2-3 days to fully clean up of 250ml of test solution using ActivGlass with area 21cm x 9 cm = 189cm^2, 0.3L_{air}/min aeration and 9.6cm between catalyst and light source.

The higher reactiveness of the mesh catalyst is in line with the theory seen in Section 2.3, as the P25 powder used to manufacture the catalyst optimises its reactiveness. Additionally, Lim's (2010) mesh catalyst also seems to have a much thicker layer of TiO_2 deposited on its surface compared to the ActivGlass. The TiO_2 coating on the mesh catalyst is also less robust mechancically and can detach from the mesh surface and move into the test solution freely, further promoting the photocatalytic degradation of the dye.

Furthermore, anaysis of the light off period (negative time) can also give a measure of the degradation associated with adsorption alone, which was found to be roughly 3%. The degradation efficiency here is very poor due to the lack of sufficient photon energy for catalyst activation. It was also observed in Figure 19 that the gradients of the curves start tailing off at the end of the first hour, suggesting that as the catalyst surface becomes increasingly saturated, the adsorption reaction slows down, before the process is reactivated again when the UV lamp is switched on at the one hour mark.

All in all, this comparison between the mesh and ActivGlass presents a tradeoff between reactivity, costs and robustness that must be considered when deliberating the use of ActivGlass for groundwater remediation and in all new reactor configuration designs.

4.4 Effects of Evaporation (Loss of Volume)

Volume Before	Volume After	Before (Time = 0)		After (Time = 14)	
		Conc Av Before		Conc Av After	Expected Conc After
100	15	**6.101**		**10.905**	**40.675**
250	160	**6.141**		**6.960**	**9.596**
500	418	**6.074**		**6.365**	**7.265**

Table 1: Changes in Concentration not due to Photocatalytic Degradation

In order to account for the effects of evaporation which were observed especially when volume of test solutions were low (~100ml), a small tank reactor test was done

without a catalyst under standard conditions ($0.3L_{air}$/min aeration, 9.6cm between catalyst and light source and one piece of ActivGlass with dimensions 21cm x 9cm) using different initial test solution volumes. Analysis of these results then enabled a correction factor to be obtained and applied to all concentration values thereafter where there is aeration.

From Table 1 above, there was a definite and significant increase in concentration of the test solution overnight. This is because evaporation of the test solution decreases the volume of water while maintaining the amount of MB hydrate in the solution mixture, thus increasing its concentration. However, as observed in Table 1 as well, the concentration after 14 hours for 100ml was calculated to be 10.905mg/L, which is within the non-linear region of the absorption-concentration calibration curve. Therefore, the results obtained for 100ml was deemed unreliable. But comparing the increase in concentration across the different volumes instead, it is clear that the increase in concentration is less for larger volumes, so their results were more reliable. The percentage decrease in volume is less significant for reservoirs of larger volume since the loss of volume was found to be almost constant across different initial volumes (85ml, 90ml and 82ml loss observed). The expected concentrations were calculated based on this reduction in volume observed. However, there was a discrepancy between the measured and calculated results, suggesting that evaporation is not the only reason for the loss of volume seen.

Initial volume	Increase in conc	Reduction in vol	Diff btw conc & vol	Increase in conc overnight (14 hours)	Increase of conc/hour
100	79%	85%	6%	**4.804**	**0.343**
250	13%	36%	23%	**0.819**	**0.058**
500	5%	16%	12%	**0.292**	**0.021**

Table 2: Analysis on the Effects of Evaporation and Reduction in Volume

Table 2 further analyses the results obtained in Table 1. It was hypothesised that only evaporation changes the concentrations of the solutions; while changes in volume due to other sources such as photolysis, air stripping etc. would remove both the water and dye together, giving no change in concentration but simply a change in volume. Therefore, the difference between the change in concentration and change in volume (gives expected change in concentration) would give the change in volume (or expected concentration) by sources other than evaporation as mentioned before. The increase of concentration per hour was also calculated, giving the correction factor required.

4.5 Effects of Solution Volume

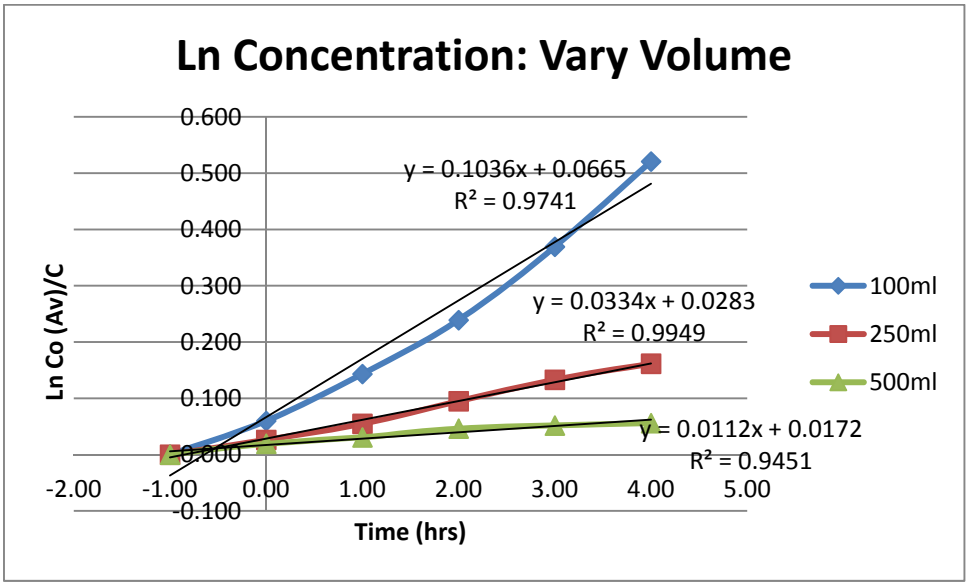

Figure 21: 5 hour Ln Concentration Curve for Different Volumes

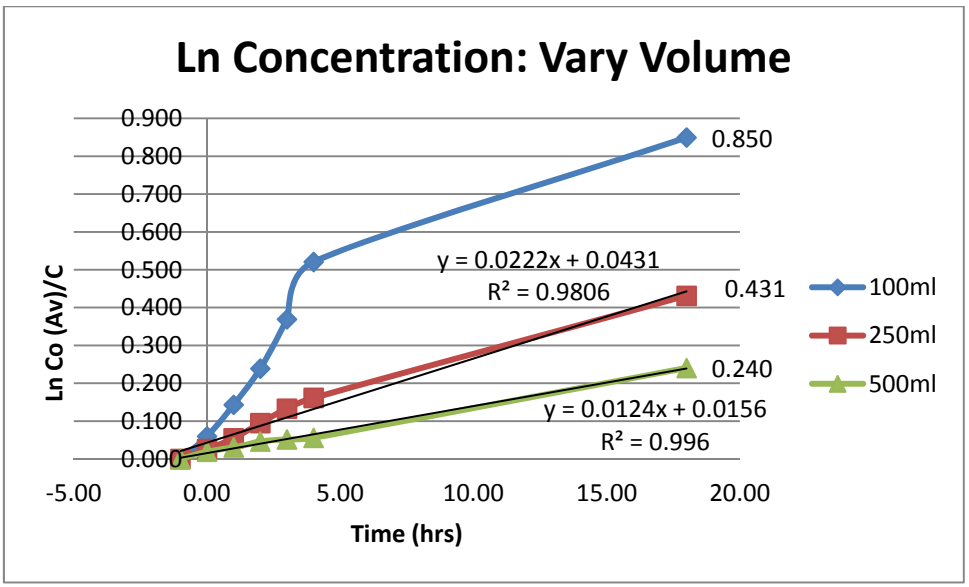

Figure 22: 19 hour Ln Concentration Curve for Different Volumes

Figures 21 and 22 show how the degradation efficiency of ActivGlass changes with the volume of solution tested after being corrected for evaporation or more accurately, lost volume effects. It was observed that the reactiveness of the ActivGlass decreases with increasing volume, which makes sense since, the larger the volume of test solution, the more pollutants that needs to be cleaned up. And since the catalyst area and distance of catalyst from the light source were kept constant, the number of hydroxyl molecules generated would have remained constant as well. But the increase in volume meant that the pollutants and the hydroxyl molecules were further apart and thus would take longer to

reach each other under the same aeration and mixing conditions. Therefore, the reactiveness decreased with increasing volume as expected theoretically. Additionally, a lower volume would also mean the photons would have to travel through less liquid which would absorb more of its energy than the air; contributing further to the observations.

After correcting for evaporation, the pseudo first order reaction assumption seemed to hold as the Ln curves for 250ml and 500ml tests were both straight lines after 5 hours and 19 hours. The Ln curve for the 100ml however was not linear; and this is especially obvious in Figure 22. This is because the loss of volume was too large for the 100ml test, making calibration and measurements inaccurate especially after the overnight period, where a pronounced change in slope can be seen. The photocatalytic degradation efficiency also seems to be inversely proportional to the volume tested because comparing the slopes and final data point for 250ml and 500ml curves in Figure 22, doubling the test volume seemed to have decreased the reaction rate by slightly more than 50%. This too is in line with theoretical expectations stating that the degradation efficiency should vary with 1/Volume.

4.6 Effects of Distance from Light Source (Irradiance)

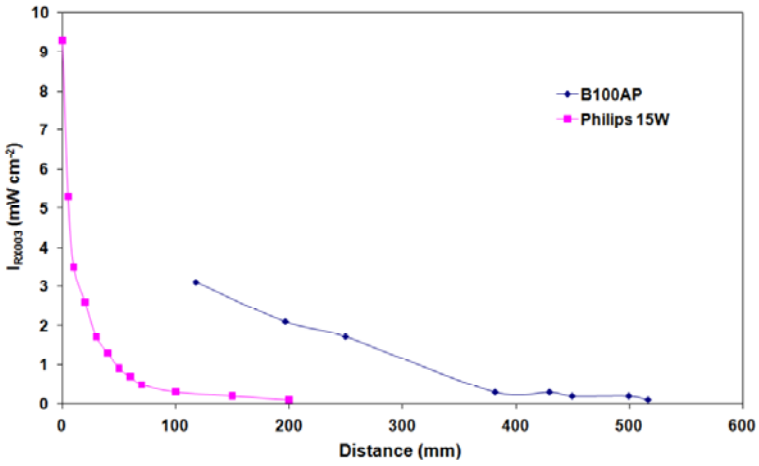

Figure 23: Variation of Light Intensity with Distance of Catalyst from Light Source (Lim, 2010)

Figure 23 from Lim (2010) shows the variation of light intensity with distance of catalyst from light source for the 15W, 365nm Philips Cleo UVA lamp used as well as for another stronger B100AP UVA lamp not used in this project measured using UVItec RX003 radiometer and light sensor with gain of 10kΩ. From the graph above, light intensity decays quite rapidly with distance for the Cleo lamp such that for the distances tested below, light intensity was much less than 1mWcm^{-2}. However, the dimensions of the small tank reactor used limited how near the catalyst could be placed to the light source during testing.

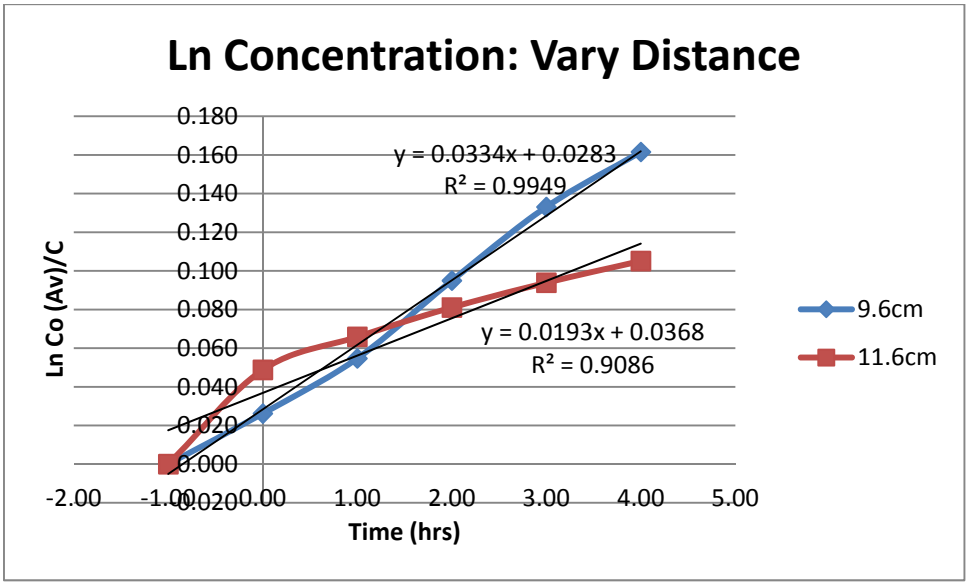

Figure 24: 5 hour Ln Concentration Curve for Different Distances

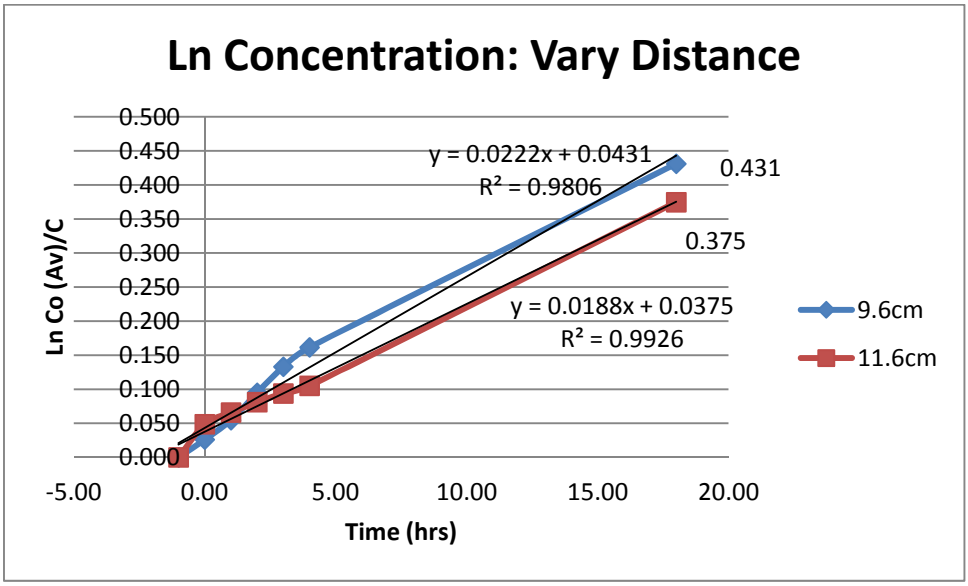

Figure 25: 19 hour Ln Concentration Curve for Different Distances

Figures 24 and 25 show how the ActivGlass reactiveness changed when the distance between the catalyst and the light source were changed (after correcting for evaporation), which, as seen from Figure 23, is an indirect way of changing the light intensity illuminating the catalyst surface. Increasing the distance between the light source and the catalyst decreased the catalyst surface light intensity which in turn reduced the number of hydroxyl radicals generated. Hence for constant catalyst area and test solution volume, the pollutants and hydroxyl molecules would once again be further apart; and so it makes sense that the reactivity of the process decreases with increasing distances.

Similar to varying volumes, Figure 25 also shows that the effect of varying distances on the photocatalytic degradation rate follows the pseudo first order assumption as well. Although in general the relationship between light intensity and distance is non-linear, it can roughly be split into 2 linear regions with a non-linear transition region in between as seen in Figure 23. The distances tested (96 and 116mm) may fall within the lower linear range of this relationship. This means that a measure of distance can be directly related to a meaure of light intensity. By comparing the slopes of the curves in Figure 25 as well as the value of the final data point, it seems to suggest that a reduction of ~17% in distance increased the degradation rate by ~13-15%, which is very close to the 17% reduction in distance. Thus, it was suggested that the photocatalytic degradation efficiency varies proportionally to light intensity, I for distances in the lower linear region (low intensity). This is in line with literature which suggests the same relationship at lower intensities as discussed in Section 2.5. At higher intensities, we expect the relationship between degradation efficiency and light intensity to change as the relationship between light intensity and distance changes to the non-linear transition region and then the higher linear region.

4.7 Effects of Flow Mixing and Oxygen (Aeration)

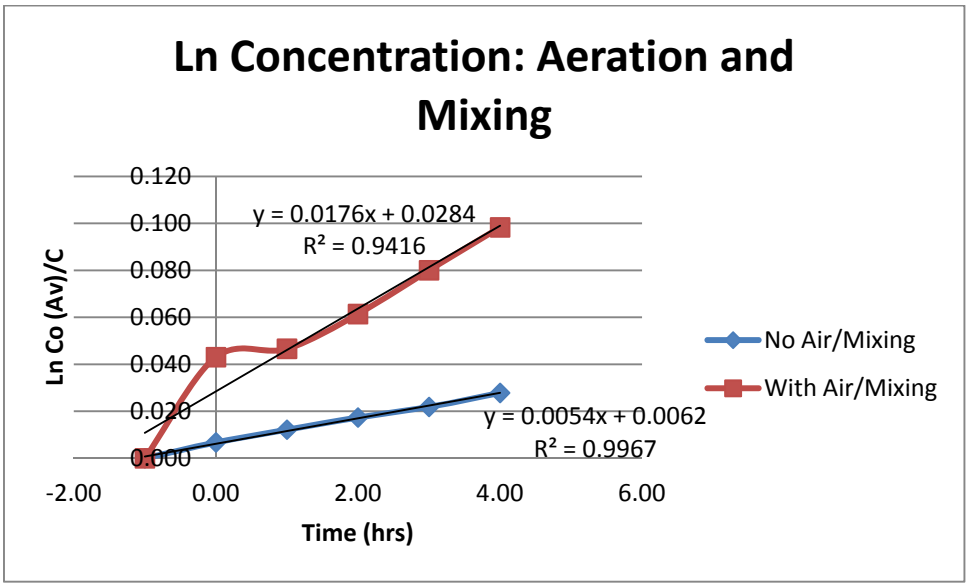

Figure 26: 5 hour Ln Concentration Curve for Different Aeration/Mixing Conditions

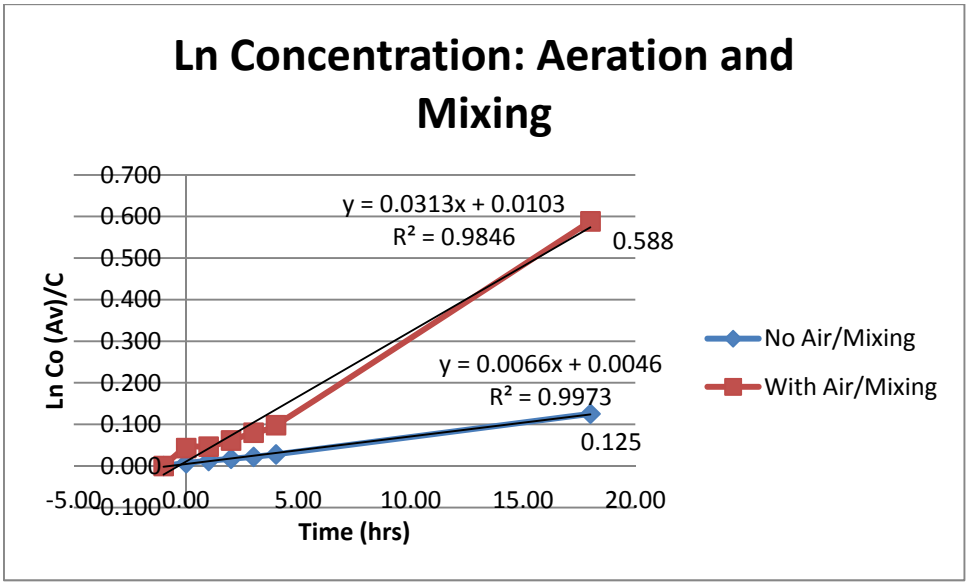

Figure 27: 19 hour Ln Concentration Curve for Different Aeration/Mixing Conditions

Previous sections in this report have highlighted numerous times the importance of oxygen for the photocatalytic degradation of contaminants. Indeed, Figures 26 and 27 clearly reiterate this as the degradation rate without aeration was very low, the lowest in fact compared to all the other tests done for this project. The aeration technique used to provide oxygen to the system also generated some mixing in the reactor, which meant that the effects of oxygen and mixing here were coupled. Aeration of the system had ensured sufficient oxygen content for the generation of hydroxyl radicals. However, although the case without aeration generated similar amounts of e_{CB}^- and h_{VB}^+, the number of hydroxyl radicals produced was significantly lower. This insufficient oxygen content meant most of the e_{CB}^- and h_{VB}^+ were forced to recombine, wasting the input light energy and decreasing reactivity significantly. Additionally, the aeration induced mixing also created localised turbulence to enhance the micro mixing of MB in the water. Shivaraju (2010) further wrote that mixing would bring the pollutants in the aqueous solution closer to the photocatalyst by decreasing the boundary layer thickness, leading to an increase in the photocatalytic degradation efficiency. Therefore, mixing has served to minimise the effect of mass transport limitation for immobilised catalyst systems (Minsker et al, 2001).

However, as the mixing and oxygen effects were coupled, it is impossible to tell just from the results here the relationship of each of these two factors with the degradation efficiency. But, their combined efforts did increase efficiency by almost 5 times. Therefore, it still makes sense to say oxygen and mixing are very important in increasing the degradation efficiency of pollutants so any proposed reactor designs should not neglect them.

4.8 Layer Test Series (Configuration Testing)

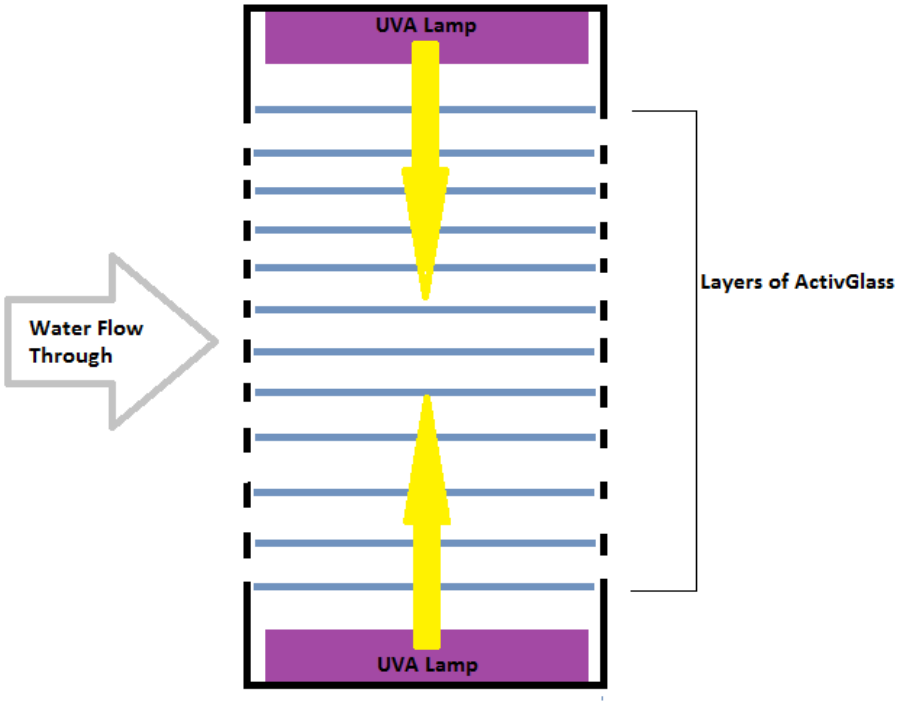

Figure 28: Proposed Layered Photocatalytic Reactor Design

The series of small tank reactor tests conducted across Sections 4.3 to 4.7 indicated that an ActivGlass reactor performs best with low solution volume, high light intensity, plus sufficient oxygen and mixing. Therefore, a layered photocatalytic reactor design as shown in Figure 28 was proposed. This configuration consists of layers of ActivGlass placed parallel to the groundwater flow direction and illuminated through perpendicularly by 2 UVA lamps at each end of the reactor. The layer test series below aim to test this configuration further to ascertain the effectiveness of degradation with light passing through layers of ActivGlass. Essentially, it hopes to deduce whether the light intensity is still sufficient for electron-hole generation in the lower layers despite the losses in light intensity after passing through layers of the glass. Additionally, this series also aims to test the effect of varying catalyst surface area on the degradation efficiency by controlling which surfaces come in contact with the test solution.

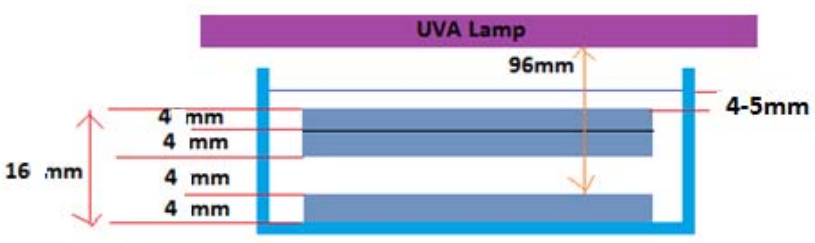

Figure 29: Measurements for Layer Test Configuration

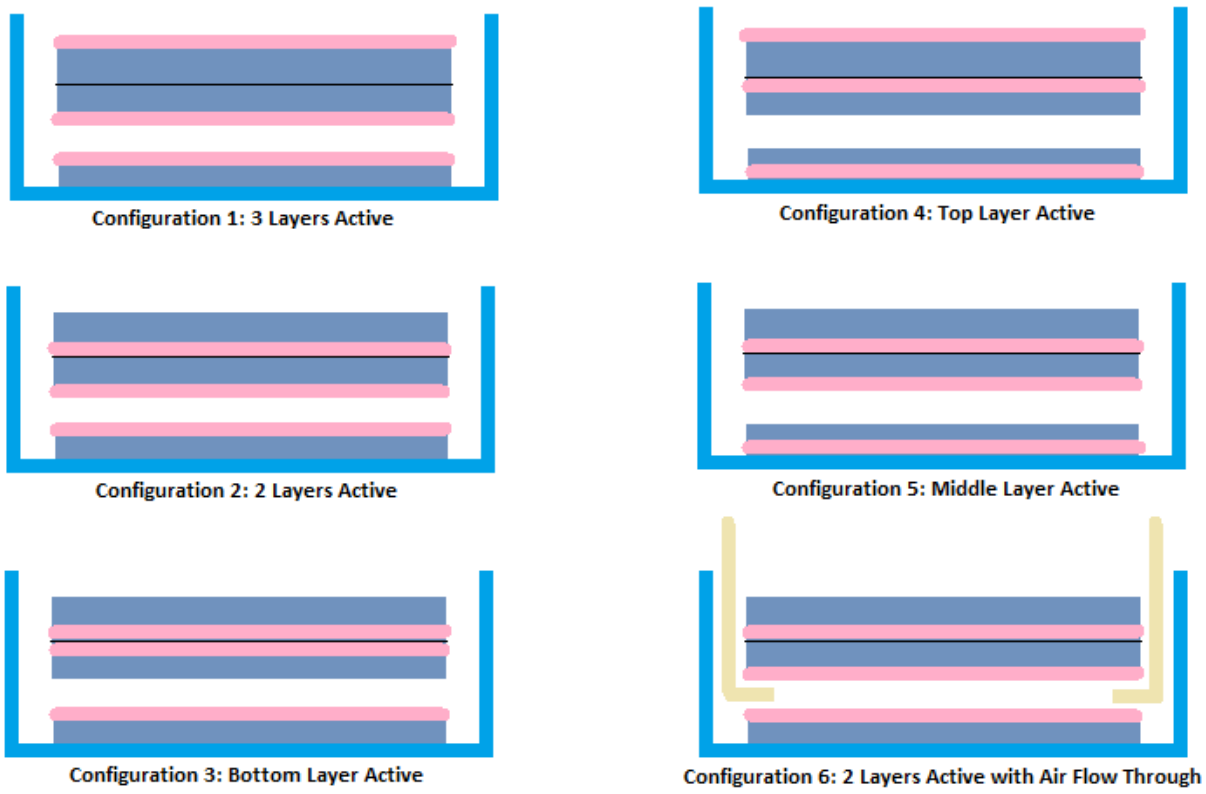

Figure 30: Schematic Drawings of the Different Layer Configurations Tested

Figure 30 above shows the different configurations tested in the layer test series. As indicated in the diagram (active sides coloured pink), Configuration 1 consists of three active layers while Configuration 2 and 6 both consist of two active layers, with the difference being Configuration 6 includes a deliberate air flow through the bottom layers to further stimulate flow mixing there. Configurations 3, 4 and 5 all have one layer being active in turn.

These tests were conducted in 3 batches: Batch 1 used new pieces of ActivGlass for testing, Batch 2 used the same pieces of glass as in Batch 1 but since a slight blue tinge was observed in the glass here, the configurations tested in Batch 2 were retested in Batch 3 using new pieces of ActivGlass. All tests utilised 250ml of test solution with $0.3L_{air}$/min aeration. The distances between each catalyst layer and the UV light source can be calculated using Figure 29. After filling the tank, the thickness of solution above the top layer of glass was about 40-50mm, which is similar to having ~100ml test solution but with catalyst much closer to the light source. The volume of solution in the gap is also similar as the gap is being propped up by small pieces of the ActivGlass of same thickness.

4.8.1 Batch Test 1: 3 Active Layers (Configuration 1), 2 Active Layers (Configuration 2) and Bottom Layer Active (Configuration 3)

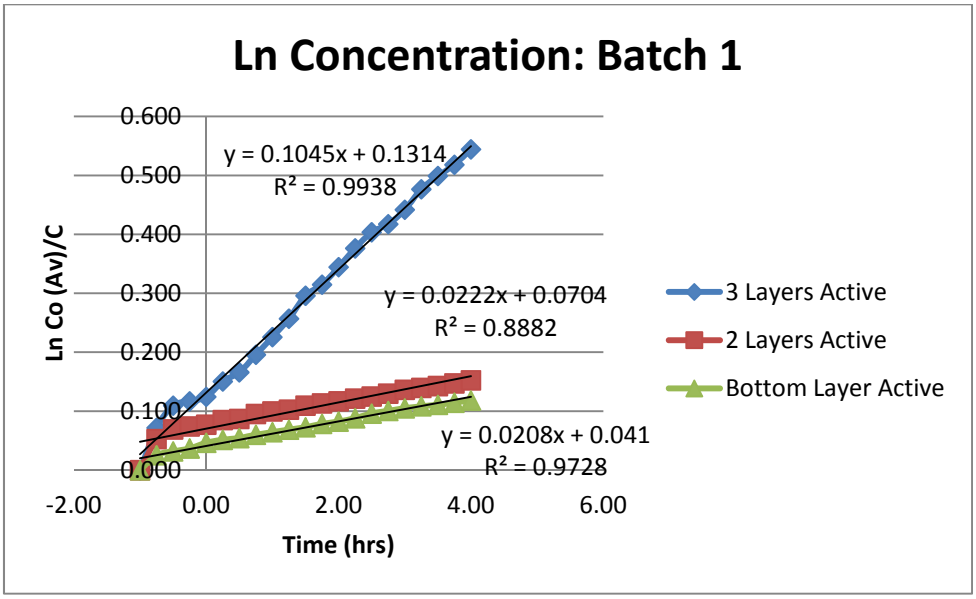

Figure 31: 5 hour Ln Concentration Curve for Batch 1 Tests (Configurations 1, 2 and 3)

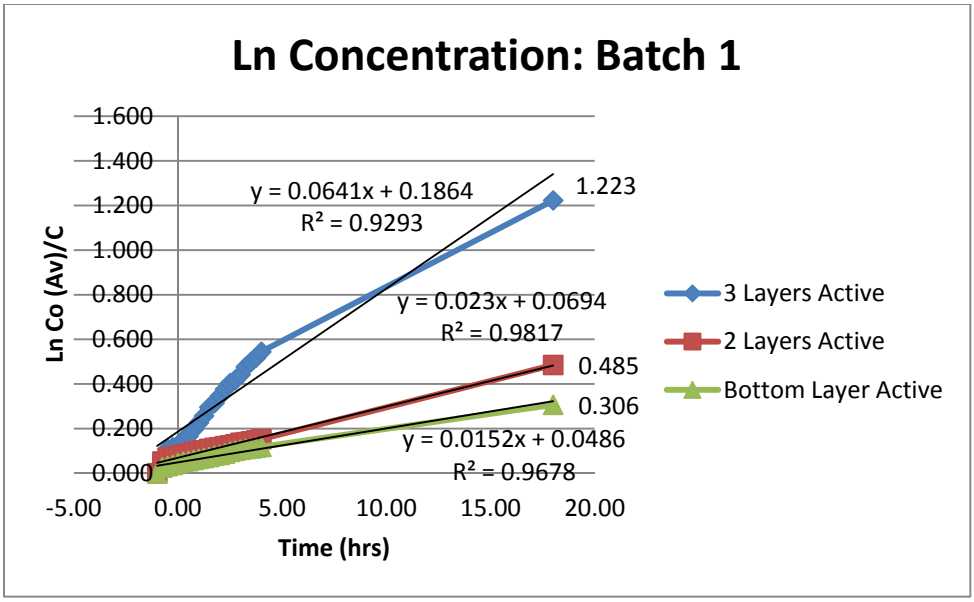

Figure 32: 19 hour Ln Concentration Curve for Batch 1 Tests (Configurations 1, 2 and 3)

Figures 30 and 31 clearly indicate that Configuration 1 works much better than Configurations 2 and 3. It was tempting to simply attribute this difference to the increase in catalyst surface area. However, if this were the case, Configuration 2 should work 2/3 times as well as Configuration 1; which in turn should work 3 times better than Configuration 3. But the observations show that Configuration 2 is only about 40% as effective as Configuration 1. Configuration 1 was also shown to be ~4 instead of 3 times more effective than Configuration 3. This suggests that there are factors on top of the increase in catalyst

surface area contributing to Configuration 1 being so much better than Configurations 2 and 3 in degrading the MB dye. The increase in catalyst surface area for a constant volume meant that each piece of ActivGlass would have to clean up less volume of the test solution, increasing the reactiveness when all three layers were active. However, even if not all three layers were active, the configuration setup still ensures that the layer of solution to be cleaned up on each surface remains low at any point in time (cleaned solution circulated so that new solution brought to catalyst surface for clean-up, maintaining same thin layer above the catalyst surface). Additionally, the distance of the catalyst from the light source is also reduced for the top and middle layers, increasing the incident light intensity on them. Hence, this suggests that most of the clean-up observed in Configuration 1 occurred in the top layer only, which is the closest to the light source. The reactiveness of the top layer alone was tested in Batch 2 and 3 to ascertain this hypothesis.

On top of that, some non-linearity was also observed for the Configuration 1 overnight test. This observation is similar to the observation for the 100ml test in Section 4.5 which further strengthens the argument that volume is kept low. However, the correction factor for evaporation used in these batch tests were for 250ml test solution as the total amount of test solution used here was 250ml. These observations though have called into question the validity of this correction factor used since the degradation process seemed more similar to the 100ml test, especially in the top layer.

4.8.2 Batch Test 2: Top Layer Active (Configuration 4), Middle Layer Active (Configuration 5) and 2 Layers Active with Air Flow Through (Configuration 6)

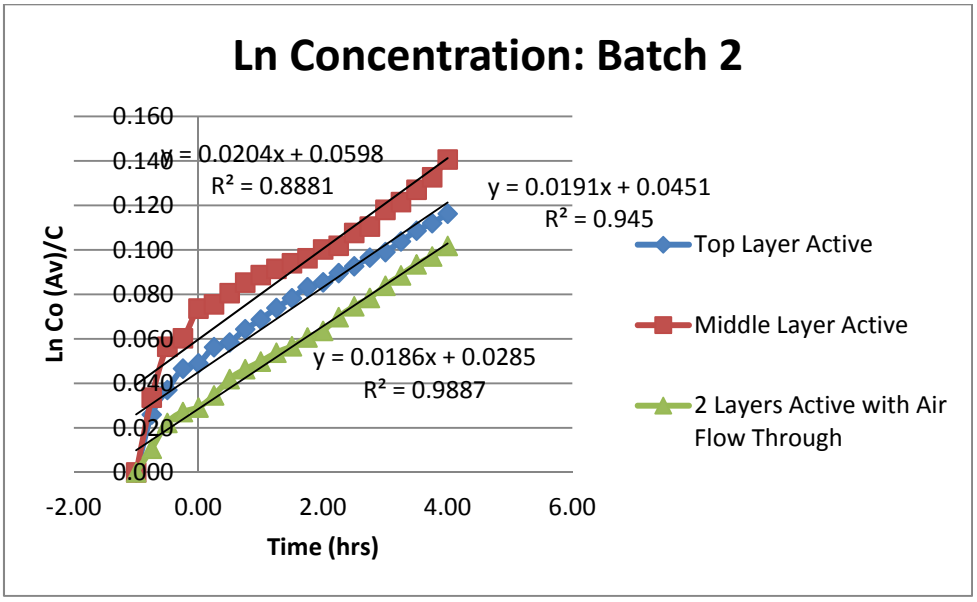

Figure 33: 5 hour Ln Concentration Curve for Batch 2 Tests (Configurations 4, 5 and 6)

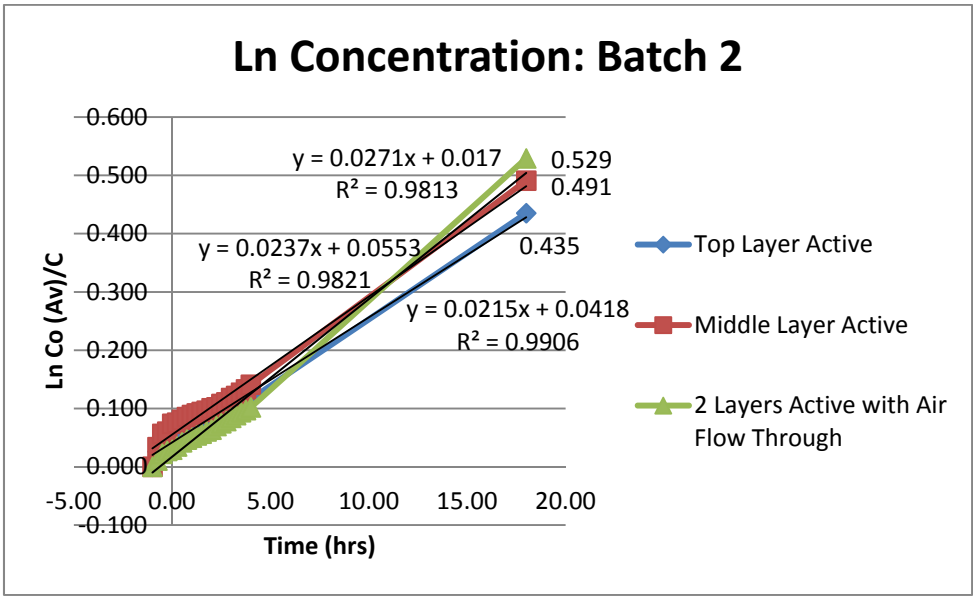

Figure 34: 19 hour Ln Concentration Curve for Batch 2 Tests (Configurations 4,5 and 6)

Following the tests done in Batch 1, some further tests were conducted in Batch 2. Configuration 4 with only the top layer active hoped to test the hypothesis that most of the clean-up in Configuration 1 is due to the top layer; while Configuration 5 hopes to deduce the effect of catalyst surface area via comparisons with Configuration 2. Configuration 5 could also be compared to Configuration 3 to show if it is possible to generate the required hydroxyl radicals through back lighting (ie photons do not hit film first but provide energy through the glass underneath). Lastly, Configuration 6 was tested because it was felt that

part of the reason why Configuration 2 did not work as well as intended was due to the fact that flow was rather stagnant in between the two lower pieces of glass (insufficient oxygen and mixing) despite having the same overall aeration rate as in previous tests. This meant that most of the mixing was likely only to be in the top layer which is the most accessible. Thus, air was deliberately flowed through this gap to ensure sufficient aeration. Unfortunately, the results obtained in Batch 2 were inconclusive and the values much smaller than expected from the ballpark numbers seen in all other tests as observed in Figures 33 and 34. This was attributed to the blue tinge observed on the glass after reuse. However, absorption testing at 365nm showed no signs of inhibited UVA transmittance at this wavelength. Thus, the blue tinge may not be due to a film of dried up solution on the catalyst surface that would block UVA light from reaching the catalyst surface, but rather the solid deposition of some MB hydrate dye particles which cannot be cleaned off the surface but perhaps doesn't stop the UVA light passing through it. These particles may have blocked off the active sites on the catalyst or hinder the production of hydroxyl radicals, culminating in a reduction of degradation efficiency when it is used. This brings into question the catalyst reuse and regeneration capacity of the ActivGlass. However, this may only be an issue associated with the use of MB dye as MTBE does not adsorb well. In conclusion, a retest was needed for the configurations tested here, as done in Batch 3.

4.8.3 Batch Test 3: Configurations 4, 5 and 6 using new pieces of ActivGlass

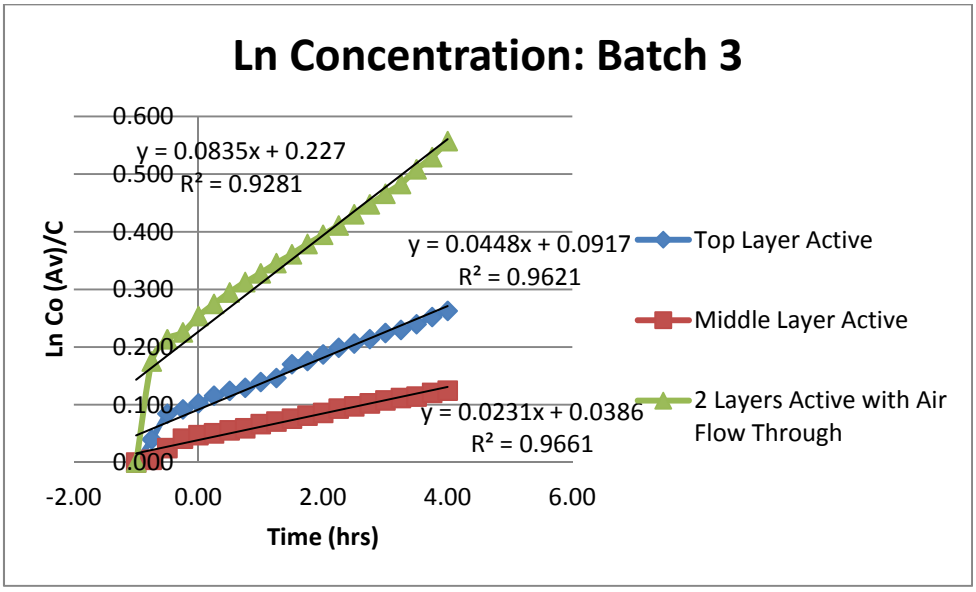

Figure 35: 5 hour Ln Concentration Curve for Batch 3 Tests (Configurations 4,5 and 6 using new glass)

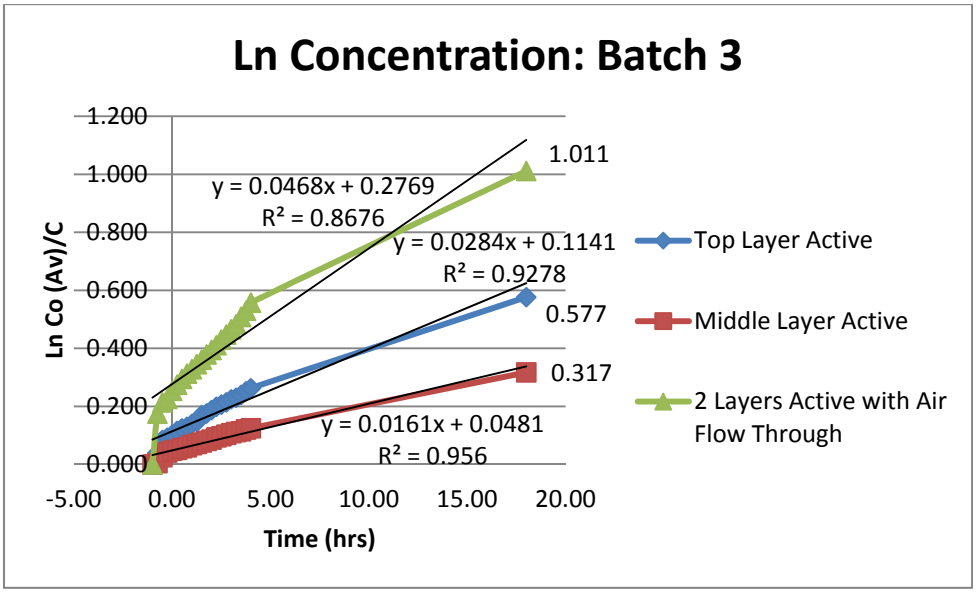

Figure 36: 19 hour Ln Concentration Curve for Batch 3 Tests (Configurations 4,5 and 6 using new glass)

Batch 3 repeats the tests done in Batch 2 but using new pieces of the ActivGlass so that the reuse capacity of the glass was no longer an issue. Figures 35 and 36 show the test results for Configurations 4, 5 and 6 under this condition. Compared to the results in Batch 2, the results here were much more in line with the results seen in Batch 1. From Figures 35 and 36, Configuration 4 (top layer active) was very active as expected; but very surprising and even better than it was how well Configuration 6 (2 layers with air flow through) performed. Configuration 6 was found to be ~3 times better than Configuration 5 and 1.6-1.8 times better than Configuration 4. Not only was there a higher catalyst surface area in Configuration 6; unlike Configuration 2, there was also sufficient mixing and aeration for the lower layers here this time. Both these factors have contributed to the higher degradation efficiency observed in Configuration 6. Further analysis and clearer comparisons between the configurations in Batch 1 and Batch 2 are detailed below in Section 4.8.4.

4.8.4 Further Comparisons Between Configurations

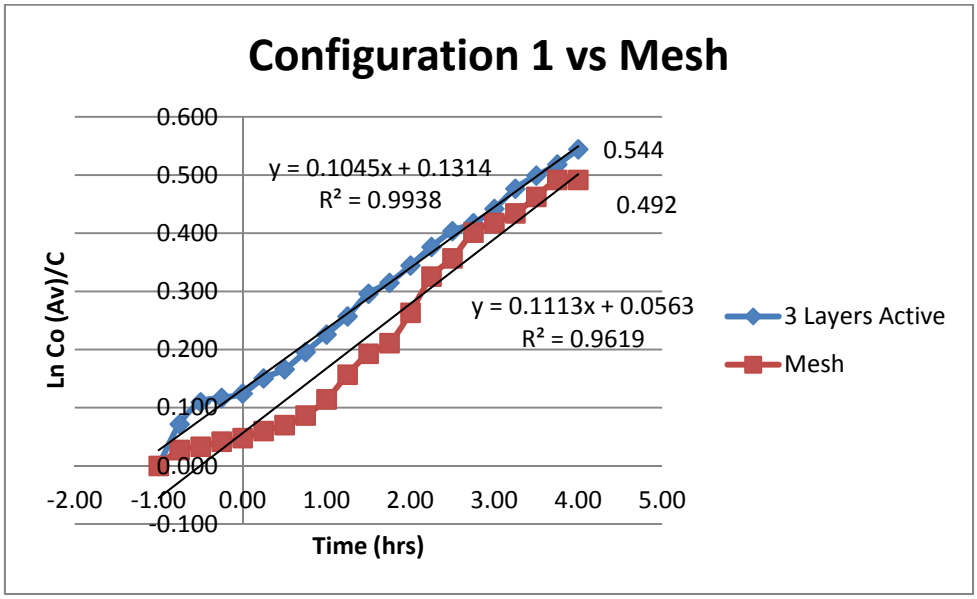

Figure 37: 5 hour Ln Concentration Curve comparing Configuration 1 and the Mesh Catalyst

Figure 37 showed that using 3 layers of ActivGlass in the configuration specified was actually as good as using 1 layer of the mesh catalyst. This further strengthens the cause and feasibility of using ActivGlass as a substitute for the mesh catalyst in groundwater remediation photocatalytic reactors. Therefore, we can expect similarly good clean-up rates with the ActivGlass as seen previously with the mesh by increasing the catalyst surface area and ensuring good mixing and aeration for small volume cleaning batches.

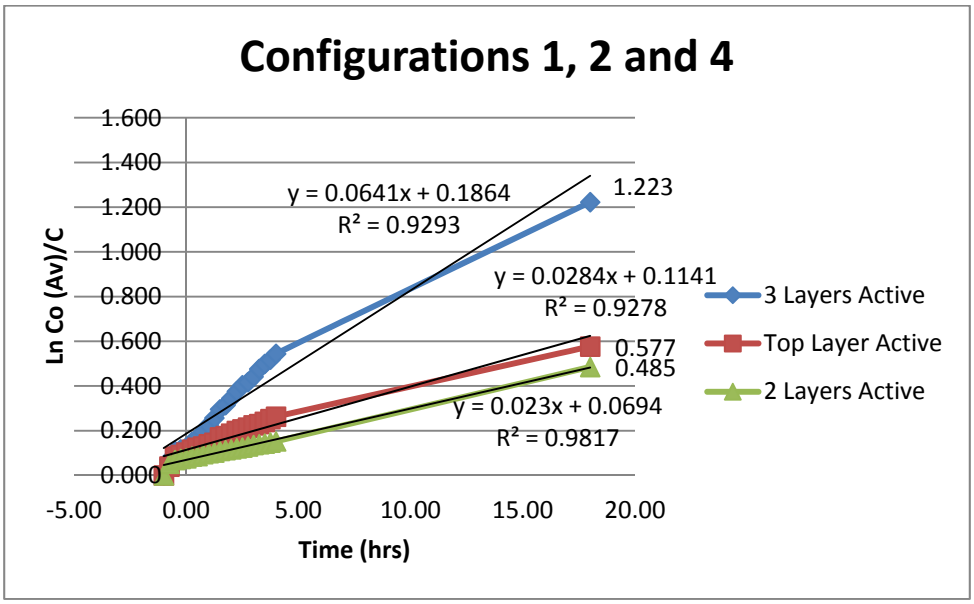

Figure 38: 19 hour Ln Concentration Curve comparing Configurations 1, 2 and 4

Next, from Figure 38, we see that the reactiveness of the configurations are additive to a certain extent. Configuration 1 could be roughly split into 2 systems shown by Configuration 2 and 4 respetively. Adding the slopes or final data points of Configurations 2 and 4 give a value of ~87% of those for Configuration 1; with the bulk coming from Configuration 4, suggesting that most of the clean-up seen in Configuration 1 did indeed come from the top layer. However, as the system is not purely additive, other unaccounted factors such as possible coupling effects between the layers of glass during the cleaning process may have contributed to the added 13% efficiency observed.

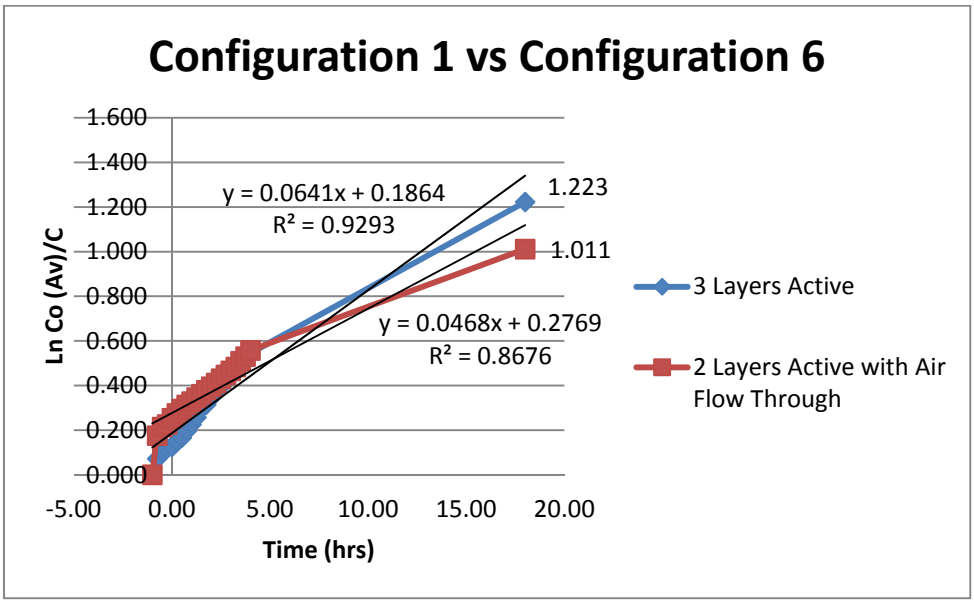

Figure 39: 19 hour Ln Concentration Curve comparing Configurations 1 and 6

The tests in Batch 3 have shown Configuration 6 to work remarkably well. Thus, comparing its reactiveness with that of Configuration 1, we see that it can clean up to ~70-80% of Configuration 1. This suggests that in our proposed reactor designs, it may be more worth it to simply just ensure good mixing and sufficient aeration instead of increasing costs by having an additional layer. Our proposed design in Figure 28 hopes to do this by keeping the gap between the pieces of glass small so that natural flow of the groundwater through the gaps will speed the flow up, ensuring sufficient turbulence.

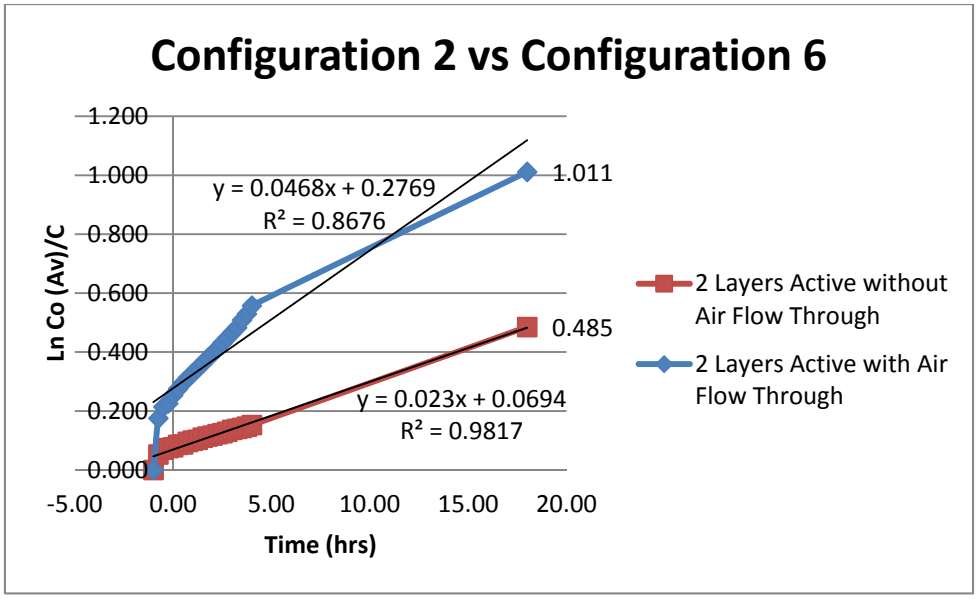

Figure 40: 19 hour Ln Concentration Curve comparing Configurations 2 and 6

Figure 40 compares more directly the effect of aeration in this layered system used. Our assumption that the flow may have been stagnant in the gap between the lower layers for Configuration 1 seemed to have been justified as there was a marked increase in degradation efficiency once aeration was deliberately introduced there. A stagnant flow meant that the cleaned solution was not brought away from the catalyst surface fast enough so further reaction can take place. Additionally, the slow degradation due to the stagnant flow also meant the concentration of the solution here may be relatively higher, resulting in less photon energy reaching the bottom layer catalyst.

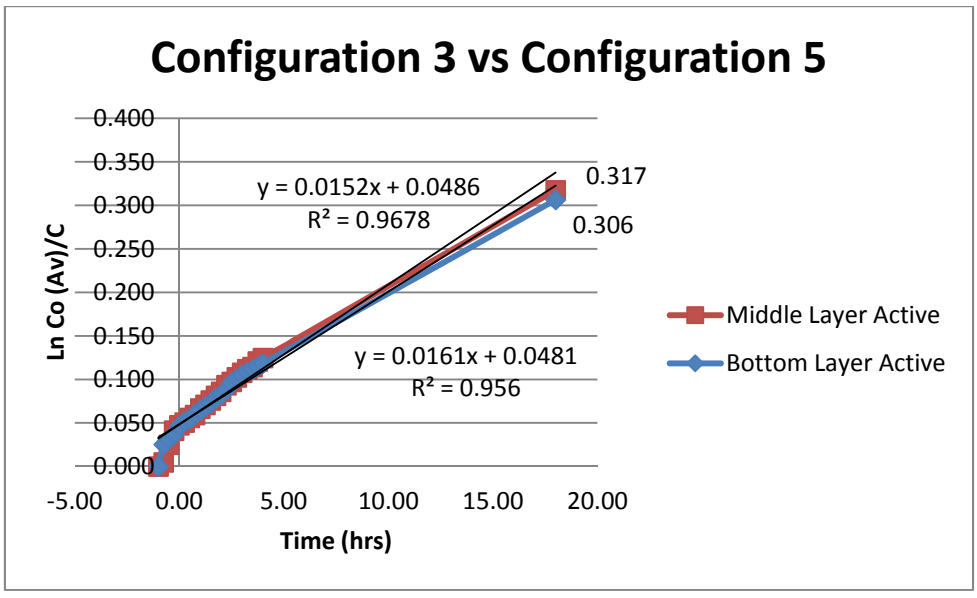

Figure 41: 19 hour Ln Concentration Curve comparing Configurations 3 and 5

Figure 41 compares the reactiveness of the middle and bottom layers to deduce whether or not it was possible to generate the required hydroxyl radicals through back lighting. As the results above show, the reactiveness of Configuration 3 and 5 are very similar, indicating that it is possible to illuminate the glass from the back and still achieve similar amounts of degradation. The degradation efficiency for the middle layer is only slightly higher than the bottom layer which can be attributed to the fact that it is 4mm closer to the light source.

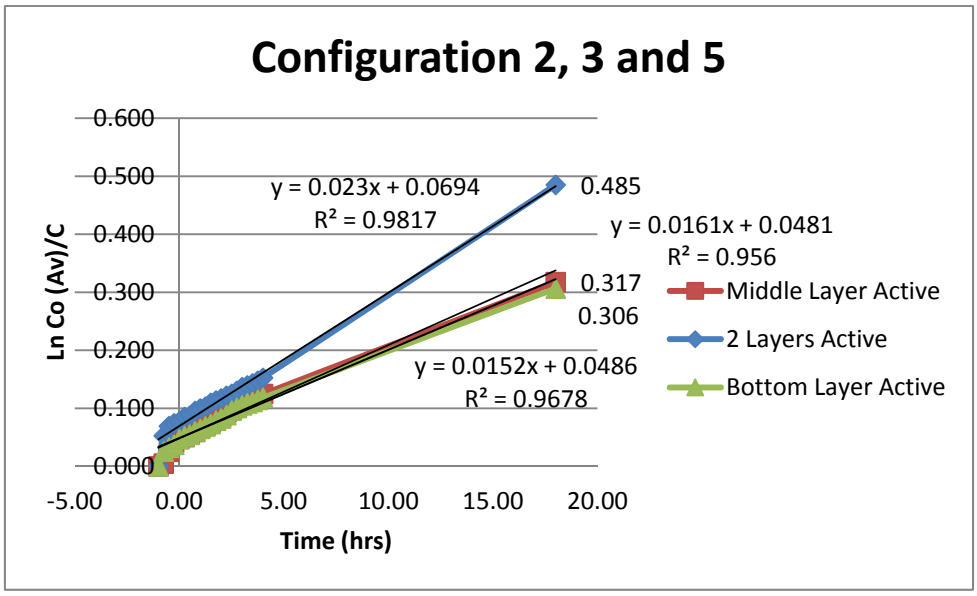

Figure 42: 19 hour Ln Concentration Curve comparing Configurations 2, 3 and 5

Comparison of Configuration 2, 3 and 5 give a clearer view of the effect of varying catalyst surface area. The similarities in the results for Configuration 2 and 5 showed that the other factors affecting the degradation rate were similar in both cases. Therefore, the additional efficiency observed for Configuration 2 must be from the increased catalyst surface area. This is in line with theory that says the degradation rate is proportional to catalyst surface area, A for a constant volume.

5 CONCLUSIONS AND SUGGESTIONS FOR FUTURE WORK

5.1 Conclusions

In conclusion, ActivGlass seems to be a good replacement for the P25 catalysts previously used in groundwater remediation, especially if multiple layers are used as in Configuration 1. The ActivGlass was found to perform best with low test solution volume, small distances from light source (high light intensity), large catalyst surface area as well as sufficient oxygen and mixing (aeration). The effects of evaporation and lost volume were also found to be significant in our experiments and a correction factor was introduced. But this should not be an issue in real life applications of groundwater treatment as the reservoir volume of solution would be large compared to the amount of volume lost. Analyses of the UV/Visible Spectra for the ActivGlass and MB dye at initial concentration found that there was a loss in transmittance of the UVA incident light when passing through layers of the glass and dye. However, the layer test series proved that this reduced intensity is still sufficient to generate enough hydroxyl radicals in the layers below for efficient degradation especially if enough oxygen and mixing were provided (Configuration 6). Furthermore, the layer test series also proved that back lighting was just as good as direct lighting in providing sufficient energy for the generation of the CB electron and VB hole pair. Thus, our proposed design that incorporates layers of ActivGlass with small gaps in between for water to flow through in order to maximise glass-pollutant contact area and keep clean-up volume low for each piece of glass seems to tick all the correct boxes based on the limiting factors tested here. However, the design did sacrifice the light intensity on the further pieces of glass. But the layer series proved that the 15W provided was sufficient for acceptable degradation at least for 3 layers.

5.2 Suggestions for Future Work

Although the results from this project drew out some important conclusions, there are still plenty of areas for further research. Firstly, a scale model of the proposed reactor design should be built and tested using not only MB dye but real pollutants like MTBE as well. The model could also be tested with other pollutants to expand the pollutant base it covers. Next, as lighting seems to be the most energy and cost intensive part of the system, more should be done to analyse alternative lighting methods, including the use of solar power and light buckets/light pipes to make photocatalytic clean-up technology even more attractive.

References

Griffiths, J. and Zabey, E. (2009), Water Facts and Trends: Version 2, *World Business Council for Sustainable Development (WBCSD)*, August 2009, ISBN 2-940240-70-1

United States Environmental Protection Agency (US EPA) (no date given), Getting Up to Speed: Groundwater Contamination, *The Magnificent Groundwater Connection Series*, adaptation of previous 1993 paper by US EPA

Lenntech Water Treatment Solutions, Sources of Groundwater Pollution, *Lenntech BV*, http://www.lenntech.com/groundwater/pollution-sources.htm, accessed May 2012

Chan, M.S.M. (2005), Photocatalytic Remediation of Organics in Groundwater, *University of Cambridge PhD Thesis*, September 2005

Lim, L.L.P. (2010), In-Situ Photocatalytic Remediation of Organic Contaminants in Groundwater, *University of Cambridge PhD Thesis*, May 2010

Deeb, R. A., Scow, K. M., Alvarez-Cohen, L. (2000), Aerobic MTBE Biodegradation: An Examination of Past Studies, *Current Challenges and Future Research Directions*

Sahle-Demessie, E., Enriquez, J., Gupta, G. (2002a), Attenuation of Methyl Tert-butyl Ether in Water using Sunlight and a Photocatalyst, *Water Environmental Resources*

Sahle-Demessie, E., Richardson, T., Almquist, C. B., Pillai, U. R. (2002b), Comparison of Liquid and Gas-phase Photooxidation of MTBE: Synthetic and Field Samples, *Journal of Environmental Engineering*

US EPA (2004), Technologies for Treating MtBE and Other Fuel Oxygenate, *US EPA/National Service Centre for Environmental Publications (NSCEP)*

Fetter, C. W. (1999), Contaminant Hydrogeology, Second Edition, *Wiley and Sons*

Mackay, D. M., Cherry, J. A. (1989), Groundwater Contamination: Pump-and-Treat Remediation, *Environmental Science & Technology*

Domenico, P. A., Schwartz, F. W. (1997), Physical and Chemical Hydrogeology, Second Edition, *John Wiley and Sons*

Bowles, M. W., Bentley, L. R., Hoyne, B., Thomas, D. A. (2000), In Situ Ground Water Remediation Using the Trench and Gate System, *Ground Water*

European Commission (2000), Directive 2000/60/EC: Establishing a Framework for Community Action in the Field of Water Policy (OJ L327)

European Commission (2006), Directive 2006/118/EC: On the Protection of Groundwater against Pollution and Deterioration (OJ L372)

Herrmann, J.-M. (2005), Heterogeneous Photocatalysis: State of the Art and Present Applications, *Topics in Catalysis*

Hoffmann, M. R., Martin, S. T., Choi, W. Y., Bahnemann D. W. (1995), Environmental Applications of Semiconductor Photocatalysis, *Chemical Reviews*

Houas, A., Lachheb, H., Ksibi, M., Elaloui, E., Guillard, C., Herrmann, J.-M. (2001), Photocatalytic Degradation Pathway of Methylene Blue in Water, *Applied Catalysis B: Environmental*

Mills, A., Davies, R. H., Worsley, D. (1993), Water Purification by Semiconductor Photocatalysis, *Chemical Society Reviews*

Barreto, R. D., Gray, K. A., Anders K. (1995), Photocatalytic Degradation of Methyl-tert-butyl-ether in TiO2 Slurries: A Proposed Reaction Scheme, *Water Research*

Chan, M. S. M., Lynch, R. J. (2003), Photocatalytic Degradation of Aqueous Methyl-tertbutyl-ether (MTBE) in a Supported-catalyst Reactor, *Environmental Chemistry Letters*

Balasubramanian, G., Dionysiou, D. D., Suidan, M. T., Subramanian, V., Baudin, I., Laine, J.-M. (2003), Titania Powder Modified Sol-gel Process for Photocatalytic Applications, *Journal of Material Science*

Li Puma, G., Yue, P. L. (2001), A Novel Fountain Photocatalytic Reactor: Model Development and Experimental Validation, *Chemical Engineering Science*

Alfano, O. M., Bahnemann, D., Cassano, A. E., Dillert, R., Goslich, R. (2000), Photocatalysis in Water Environments using Artificial and Solar Light, *Catalysis Today*

Almquist, C. B., Sahle-Demessie, E., Enriquez, J., Biswas, P. (2003), The Photocatalytic Oxidation of Low Concentration MTBE on Titanium Dioxide from Groundwater in a Falling Film Reactor, *Environmental Progress*

Robert, D., Malato, S. (2002), Solar Photocatalysis: A Clean Process for Water Detoxification, *The Science of the Total Environment*

Mehos, M. S., Turchi, C. S. (1993), Field Testing Solar Photocatalytic Detoxification on TCE contaminated groundwater, *Environmental Progress*

Bahnemann, D. (2004), Photocatalytic Water Treatment: Solar Energy Applications, *Solar Energy*

Peill, N. J., Hoffmann, M. R. (2000), TiO2-coated Fibre Optic Cable Reactor, *US Patent 6051194*

Ray, A. K., Beenackers, A. A. C. M. (1998a), Development of a New Photocatalytic Reactor for Water Purification, *Catalysis Today*

Ray, A. K., Beenackers, A. A. C. M. (1998b), Novel Photocatalytic Reactor for Water Purification, *AIChE Journal*

Dionysiou, D. D., Burbano, A. A., Suidan, M. T., Baudin I., Laine, J.-M. (2002), Effect of Oxygen in a Thin-film Rotating Disk Photocatalytic Reactor, *Environmental Science & Technology*

Bhatkhande, D. S., Pangarkar, V. G., Beenackers, A. A. C. M. (2001), Photocatalytic Degradation for Environmental Applications – A Review, *Journal of Chemical Technology & Biotechnology*

Ryu J. H., Choi, W. Y. (2008), Substrate-specific Photocatalytic Activities of TiO2 and Multiactivity Test for Water Treatment Application, *Environmental Science & Technology*

Agustina, T. E., Ang, H. M., Vareek, V. K. (2005), A Review of Synergistic Effect of Photocatalysis and Ozonation on Wastewater Treatment, *Journal of Photochemistry and Photobiology C: Photochemistry Reviews*

Matthews, R. W. (1992), Photocatalytic Oxidation of Organic Contaminants in Water: An Acid to Environmental Preservation, *Pure and Applied Chemistry*

Lim, L. L. P., Lynch, R. J. (2010a), A Proposed Photocatalytic Reactor Design for In-situ Groundwater Applications, *Applied Catalysis A: General*

Alfano, O. M., Cabrera, M. I. and Cassano, E. (1997), Photocatalytic Reactions Involving Hydroxyl Radical Attack I. Reaction Kinetics Formulation with Explicit Photon Absorption Effects, *Journal of Catalysis*

Brown, G. E., Henrich, V. E., Casey, W. H., Clark, D. L., Eggleston, C., Felmy, A., Goodman, D.W., Gratzel, M., Maciel, G., McCarthy, M. I., Nealson, K. H., Sverjensky, D.A., Toney, M. F. and Zachara, J.M. (1999), Metal Oxide Surfaces and Their Interactions with Aqueous Solutions and Microbial Organisms, *Chemical Review*

Won, D. J., Wang, C. H., Jang, H. K. and Choi, D.J. (2001), Effects of Thermally Induced Anatase-to-Rutile Phase Transition in MOCVD-grown TiO_2 Films on Structural and Optical Properties, *Applied Physics A*

Choi, W.Y. and Hoffmann, M. R. (1997), Novel Photocatalytic Mechanism for CHC13, CHBr3 and CC13CO2 – Degradation and the Fate of Photogenerated Trialomethy Radicals on TiO2, *Environmental Science and Technology*

Rideh, L., Wehrer, A., Ronze, D. and Zoulalian, A. (1997), Photocatalytic Degradation of 2-Chlorophenol in TiO2 Aqueous Suspension: Modeling of Reaction Rate, *Ind Eng Chem Res*

Davis, A. P. and Green, D.L. (1999), Photocatalytic Oxidation of Cadmium EDTA with Titanium Dioxide, *Environmental Science and Technology*

Chen, A., Lu, G., Tao, Y., Dai, Z. and Gu, H. (2001), Novel Photocatalyst Immobilised on Springs and Packed Photoreactors, *Mater Phys Mech*

Mills, A., Lepre, A., Elliott, N., Bhopala, S., Parkin, I. P. and O'Neill, S. A. (2003), Characterisation of the photocatalyst Pilkington ActivTM: a reference film photocatalyst?, *Journal of Photochemistry and Photobiology*

Chan, M. S. M., Lynch, R. J., Rolt, S. (2006), Design of Underground Photocatalytic Reactor for Borden Test, *University of Cambridge, U. K. (unpublished work)*

Chin, P. and Ollis, D. F. (2007), Decolorization of organic dyes on Pilkington ActivTM photocatalytic glass, *Catalysis Today*

Lim, L. L. P. and Lynch, R. (2010), Hydraulic performance of a proposed in situ photocatalytic reactor for degradation of MTBE in water, *Chemosphere*

US EPA (1999), Multi-Phase Extraction: State-of-the-Practice

Pilkington Glass Company, Pilkington Activ Self-Cleaning Window Glass, accessed May 2012, http://www.pilkington.com/products/bp/bybenefit/selfcleaning/default.htm

Appendix

After completing this project, it was felt that the tests conducted were very safe and there were minimal issues mostly due to the simplicity of the procedures. Therefore, there were no additional safety issues to be reported on top of the risk assessment done prior to the start of the project